الجمهورية الجزائرية الديمقراطية الشعبية
Democratic and Popular Republic of Algeria
وزارة التعليم العالي و البحث العلمي
Ministry of Higher Education and Scientific Research

جامعة زيان عاشور بالجلفة
Ziane Achour University of Djelfa

كلية العلوم و التكنولوجيا
Faculty of Science and Technology

Department: Electrical Engineering

Order N°: 008 /2020

Defense authorization N°: 192 / 2020

Laboratoire Modélisation Simulation et Optimisation des Systèmes Complexes Réels (MSOSCR)

DOCTORAL THESIS

Presented by:

Mr Nail ALAOUI

With a view to obtaining the doctoral degree in 3rd Cycle Doctoral (D-LMD)

Branch: Electronic

Specialty: Signal image and systems

Title

Image Filtering Based on Evolutionary Algorithms

Supported, on: 10/10/2020, before the jury composed of:

Full Name	Grade	Institution of affiliation	Designation
Mr Omar MANSOUR	Professor	University of Djelfa	President
Mrs Amal Baha Houda ADAMOU-MITICHE	Professor	University of Djelfa	Supervisor
Mr Lahcène MITICHE	Professor	University of Djelfa	Examiner
Mr Benharrat BELAIDI	Professor	University of Mostaganem	Examiner
Mr Mohamed Lamine TALBI	MCA	University of Bordj Bou Arreridj	Examiner

Djelfa University, FST- 2020

الجمهورية الجزائرية الديمقراطية الشعبية
République Algérienne Démocratique et Populaire
وزارة التعليم العالي و البحث العلمي
Ministère De L'enseignement Supérieur et De La Recherche Scientifique

جامعة زيان عاشور بالجلفة
Université Ziane Achour de Djelfa

كلية العلوم و التكنولوجيا
Faculté des Sciences et Technologies

Département : Génie électriques

Order N°: 008/2020

Défendu Autorisation N°: 192/ 2020

Laboratoire Modélisation Simulation et Optimisation des Systèmes Complexes Réels (MSOSCR)

THÈSE DE DOCTORAT

Présenté par :
Mr Nail ALAOUI

En vue de l'obtention du diplôme de Docteur en 3éme cycle (D-LMD)
Branche : Électronique
Spécialité : Signal image et systèmes

Titre

Filtrage D'image Basée Sur Les Algorithmes Évolutionnaires

Défendu publiquement, le 10/10/2020, devant le jury composé de :

Nom et Prénom	Grade	Institution d'affiliation	Désignation
Mr Omar MANSOUR	Professeur	Université de Djelfa	Président
Mme Amal Baha Houda ADAMOU-MITICHE	Professeure	Université de Djelfa	Directeur de Thèse
Mr Lahcène MITICHE	Professeur	Université de Djelfa	Examiner
Mr Benharrat BELAIDI	Professeur	Université de Mostaganem	Examiner
Mr Mohamed Lamine TALBI	MCA	Université de Bordj Bou Arreridj	Examiner

Université de Djelfa, FST- 2020

Dedication

قال تعالى

{ يَرْفَعِ اللَّهُ الَّذِينَ آمَنُوا مِنكُمْ وَالَّذِينَ أُوتُوا الْعِلْمَ دَرَجَاتٍ}

[المجادلة الآية 11]

Dedication

This thesis work is dedicated to:

My parents.
All of my family,
anyone he likes me. I hope that Allah will preserve them and give them
health and wellness.
All the teachers of the Electrical Engineering
Department of the University Ziane Achour of Djelfa.
- To the ALAOUI and CHELLALI families.
- My colleagues from the doctorate.
My friends.

Nail Alaoui
Djelfa on: 26/01/2020

Acknowledgement

Acknowledgement

I would first like to thank ALLAH almighty for giving me the strength and then the patience to complete my thesis.

I would like to sincerely thank my supervisor. Pr. ADAMOU-MITICHE Amal Baha Houda who helped to do everything from the beginning of the project idea to the last step in it, which enabled me to improve and understand the topic. Without his invaluable advice, this work would not have been possible.

I am very grateful for the Pr. MITICHE Lahcène, for his encouragement, supervision and support.

I want like to thank the jury members honored me with their participation in the defense.

Pr. Omar MANSOUR

Pr. Benharrat BELAIDI

Dr. Mohamed Lamine TALBI

Finally, thank you to everyone who contributed, from near or far, to achieving this work

Table of Contents

Chapter III: Effective Hybrid Genetic algorithm -proposed algorithm-

Chapter IV: Applications, results and Discussions

List of Tables

Table page

List of figures

Figure page

Lists of Acronyms and Symbols

AA MODEL	Aubert And Aujol
ACO	Ant Colony Optimization
AMF	Adaptive Median Filter
AWMF	Adaptive Weighted Mean Filter
BPDF	Based on Pixel Density Filter
DAMF	Different Applied Median Filter
DBA	Decision-Based Algorithm
DE	Differential Evolution
EA	Evolutionary Algorithm
EAs	Evolutionary Algorithms
EC	Evolutionary Computing
EHGA	Effective Hybrid Genetic Algorithms
EP	Evolutionary Programming
EPI	Edge Preservation Index
ES	Evolution Strategy
GA	Genetic Algorithm
GAs	Genetic Algorithms
GP	Genetic Programming
HGA	Hybrid Genetic Algorithm
IEF	Image Enhancement Factor
IQI	Image Quality Index
MAE	Mean Absolute Error
MDBUTMF	Modified Decision-Based Unsymmetrical Trimmed Median Filter
MF	Median Filter
MRI	Magnetic Resonance Imaging
MSE	Mean Squared Error
NAFSM	Noise Adaptive Fuzzy Switching Median Filter
ND	Noise Density

NDs	Noise Densities
PDE	Partial Differential Equations
PSNR	Peak Signal to Noise Ratio
PSO	Particle Swarm Optimization
RVIN	Random-Valued Impulse Noise
SI	Swarm Intelligence
SNR	Signal-To-Noise Ratio
SPN	Salt and Pepper Noise.
SSIM	Structural Similarity Index
TV	Total Variation
UQI	Universal Quality Index
VIF	Visual Information Fidelity
WS	Window Size

General Introduction

Introduction

Images have long ceased to be just memories and have become indispensable in many areas. Medicine [1], astronomy [2], physics [3], biology [4] among others are just some of the areas where the use of images made great strides. The use and even popularization of digital images in various areas has created new challenges in its use. For example, only one social network, Facebook, estimated that by September 2013 its users uploaded an average of 350 million images per day [5]. Despite several technological advances, digital images have intrinsic noise to them that can be caused by several factors, such as limitation of the sensors used for image acquisition, imperfections in the used lens, problems during the transmission and compression processes. among others. The problem of noise suppression or attenuation in images deals with these cases, seeking to reduce the amount of noise present in the image while preserving important features such as edges, corners and textures [6]. Noise suppression techniques have been intensively researched in the literature [7], [8] and applied to several real problems [9], however, there is still no definitive solution to this problem. This means that there is still room for improvements on existing approaches and for the proposition of new ideas, so motivating the present work to introduce a hybrid genetic algorithm (HGA) for removing a salt and pepper noise in the image. Genetic Algorithms (GA) are metaheuristics based on the concepts of natural selection, where the fittest individual tends to survive and reproduce most likely [10]. In this context, an individual is a representation of the solution of the problem addressed. Robust exploration of the search space for possible solutions make GAs an option for applications in many areas [11]–[13].

This work proposes an Effective Hybrid Genetic Algorithm (EHGA) for noise reduction in images corrupted by a salt and pepper noise. It combines a genetic algorithm with three noise suppression methods: Noise adaptive fuzzy switching median filter (NAFSM) [14], different applied median filter (DAMF), [15] and a new adaptive weighted mean filter (AWMF) [16]. The strength of the evolutionary approach is used to exploit the solution space, while image

retrieval methods are used to enhance the solutions created. EHGA is compared with other methods in the literature using corrupted benchmark images with different noise densities (NDs) for is salt and pepper noise (SPN). Medical images corrupted with an SPN noise are also evaluated. The results show that the EHGA was able to generate better quality restored images than other methods in the literature in several cases.

Motivation and Problem Statement

From the assumptions already attested above, which indicate the ability of genetic algorithms to move through a search space in search of good solutions for a given problem, it is expected that an approach with this inspiration would have good results in solving a problem as important as image denoising. To this end, the present thesis proposes the use of an Effective Hybrid Genetic Algorithm (EHGA) to solve the problem of noise suppression in images. The main points to be addressed are:

1. Study of the problem of image denoising in digital images.
2. Proposition and application of an Effective Hybrid Genetic Algorithm that combines GA with image denoising methods.
3. Evaluation results in EHGA when compared to existing methods in the literature.
4. The application of the proposed algorithm in medical images.

The hypothesis to be verified during this work is that the proposed technique is capable of finding good quality solutions when compared with other known methods for the suppression of noise in grayscale images.

Thesis outline

This work is organized as follows:

- The first chapter is a reminder of some basic definitions concerning the Evolutionary algorithm (EA), overview of Genetic Algorithms (GAs) and other evolutionary algorithms (EAs).
- The second chapter presents the literature review presenting the state of the art of noise suppression methods in images.

- The third chapter presents the theoretical framework used as the basis of the proposed method as well as the proposed EHGA, and details their main features and how they work.
- The fourth chapter shows the results obtained by EHGA in various performed tests.
- The fifth chapter is the conclusions drawn in this paper.

CHAPTER I

Background on Evolutionary Algorithms

I.1 Introduction

This chapter gives the reader through this thesis the fundamentals for the study of evolutionary computing (EC). We begin with a definition of evolutionary algorithm and provide to an overview of the biological processes that have motivated researchers and given them a rich source of ideas and metaphors to be inspired. The main components of genetic algorithms will be addressed. The function and associated technical problems will be clarified. We conclude with descriptions of other algorithms in evolution.

I.2 Evolutionary algorithms

An evolutionary algorithm (EA) is a subgroup of an evolutionary computation a generic population-based metaheuristic optimization algorithm in Artificial Intelligence (AI). An EA uses mechanisms inspired by biological evolution, such as representation, mutation, crossover, and selection. Candidate solutions to the optimization problem play the role of individuals in a population, and the fitness function determines the quality of the solutions. The evolution of the population then takes place after the repeated application of the above operators **[17]**, **[18]**. Similar algorithms differ in genetic representation and other implementation details, and the nature of the particular applied problem.

I.2.1 Genetic algorithm

I.2.1.1 Overview of Genetic Algorithms

Genetic algorithms are heuristic search strategies accessible to a broad range of optimization problems. Such simplicity allows them to be attractive in action to many optimization problems. Genetic algorithms are based on evolution. A good reason to believe in the power of nature is the modern organisms, diversity and performance. Species may adjust to their environment. **[19]**.

Algorithm **1** and Figure **I.1** are able to describe the classic or basic genetic algorithm as suggested by Holland **[20]**. Individuals are created randomly and their chromosomes are encoded with binary strings. Different and new entities are produced and introduced to the population by recombination and mutation operations. The operators and the parent selection will be explained in Algorithm **1**.

Algorithm 1 Basic Genetic Algorithm.

1: Generate initial population randomly;
2: Calculate the fitness of individuals in the population;
3: **Repeat**
4: Select parents;
5: Crossover with selected parents;
6: Mutate the children generated in the previous operation;
7: Calculate children's fitness;
8: Replace all individuals in the current population with children;
9: **Until** termination condition

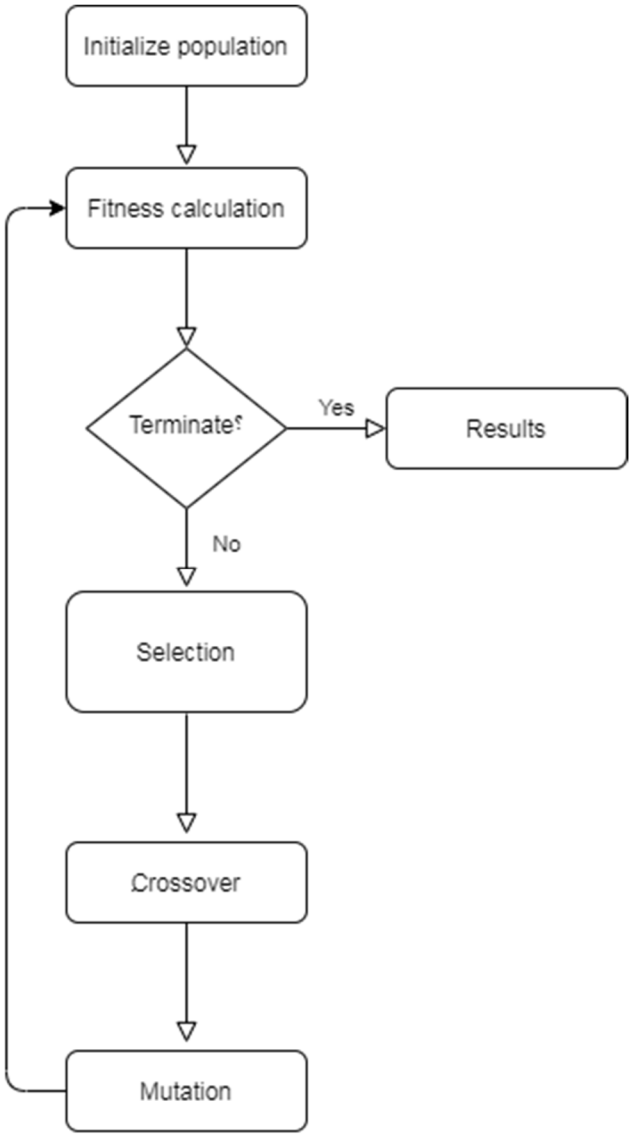

Figure I.1 : Diagram depicting the steps performed by a Genetic Algorithm

I.2.1.2 Representation and evaluation

The chromosome has multiple representations and the preference of the right representation is problem-specific. The good description renders the search area narrower and therefore an easier search. For the chromosome, representations are binary, permutation, value is available. Each part of the chromosome is called a gene.

After all chromosomes have been identified, the right way optimization is to scan the space to measure every individual's fitness value. The fitness value of a chromosome is determined in a process called evaluation. After getting how to represent each individual, the next step is initializing the population by selecting the proper number of individuals within it.

I.2.1.3 Selection

The principal procedures for parent selection take into consideration the fitness of every individual in the population. The most important forms are by ranking, tournament and roulette selection [21], [22]:

- **In the selection by ranking**, each individual is rated according to its fitness and the likelihood of selection of each individual is decided by its classification within the ranking.

- **In the tournament selection** Figure I.2, a number of individuals from the population are randomly selected and the fittest among them is chosen for reproduction. The process is repeated until the required number of parents is reached.

- **In roulette selection** Figure I.3, it is possible that all individuals in the population would be chosen for reproduction, although depending on their fitness, the possibility of selection differs.

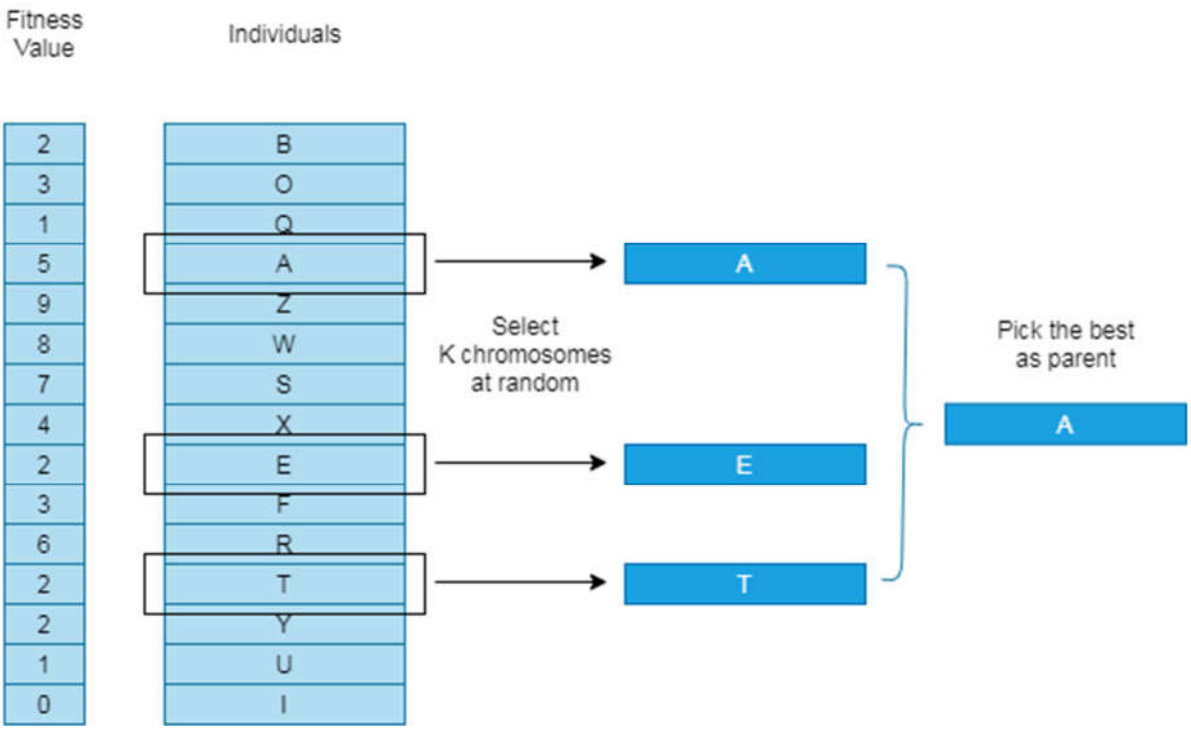

Figure I.2 : Example of tournament selection.

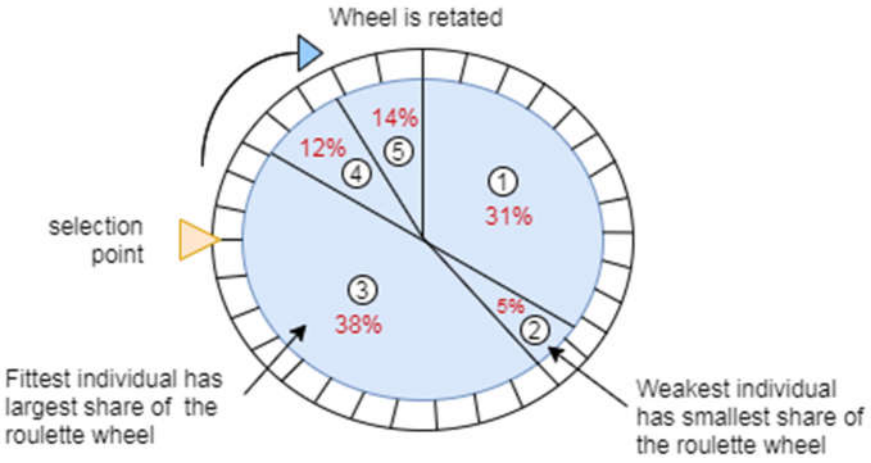

Figure I.3 : Example of roulette selection.

I.2.1.4 Crossover operators

Crossover, also referred to as recombination is the process by which the children are created from the selected parents [22], in other words through information exchange to provide a different new interpretation of the solution (individual). There are different ways to recombine, but the overall aim is to ensure that children have their first parent chromosome and a second parent chromosome. Typically, recombination takes place at a certain probability rate identified by the problem's need.

Some popular crossover strategies are the 1-point crossover, which draws a location and shapes a child by the initial sequence of the first parent and the final sequence of the second parent. The second child is created analogously from the initial sequence of the second parent and the end of the first parent. The n-point crossover operates analogously with the 1-point crossover, but n cutoffs are drawn instead of a cutoff. Every child element is granted a 50% likelihood of belonging to the first or second parent by a uniform crossover. In Figures I.4, I.5 and I.6 respectively all three forms of recombination are highlighted.

New representations have been proposed for GAs, where individuals are represented by integers and reals with specific recombination operators. For example, on the average crossover the child value is calculated from the average of the parent values. In arithmetic crossover, the child value is calculated as a point on the line between the parent values.

- **1-point crossover.**

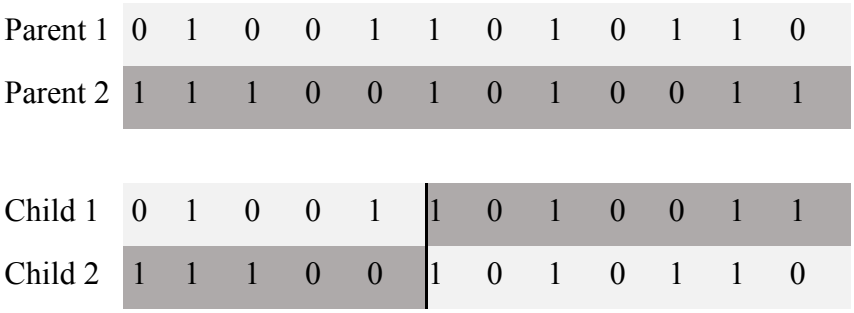

Figure I.4 : 1-point crossover.

- **2-point crossover.**

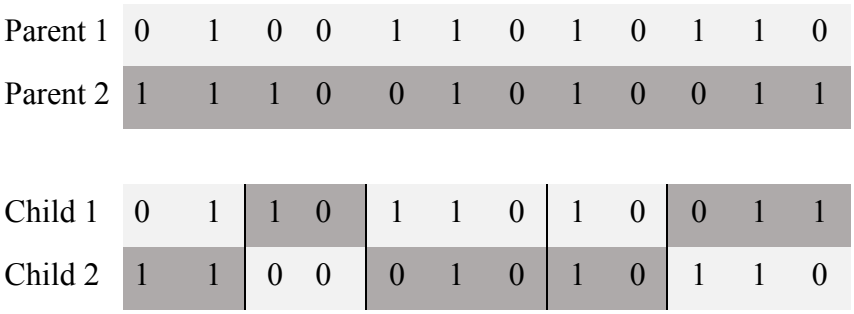

Figure I.5 : 2-point crossover.

- **Uniform crossover.**

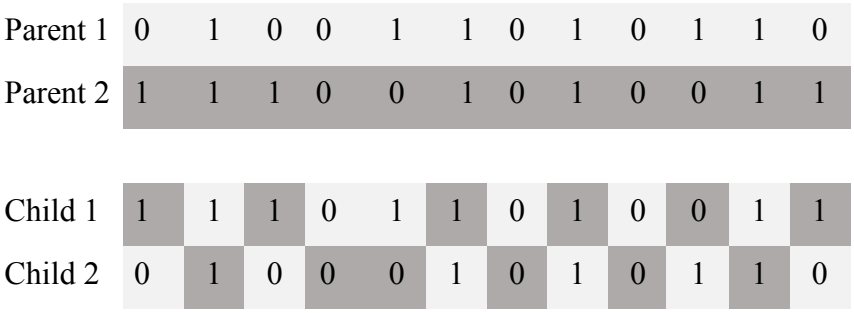

Figure I.6 : Uniform crossover.

- **Whole Arithmetic Recombination**

This is commonly used for integer representations and works by taking the weighted average of the two parents by using the following formulas as shown in Figure I.7.

Child1 = α.x + (1-α). y

Child2 = α.x + (1-α). y

x, y are the parents. Obviously, if α = 0.5, then both children will be identical as shown in the following image

Parent 1	0.1	0.1	0.2	0.2	0.3	0.3	0.4	0.4	0.5	0.5	0.6	0.6
Parent 2	0.2	0.3	0.2	0.2	0.2	0.3	0.3	0.2	0.3	0.2	0.4	0.4
Child 1	0.15	0.2	0.2	0.2	0.25	0.3	0.35	0.3	0.4	0.35	0.5	0.5
Child 2	0.15	0.2	0.2	0.2	0.25	0.3	0.35	0.3	0.4	0.35	0.5	0.5

Figure I.7 : Whole Arithmetic Recombination.

I.2.1.5 Mutation operators

The mutation is a mechanism that applies changes to the chromosome of an individual. The goal is to help preserve the population's diversity. As with recombination, a certain probability rate is also used for the mutation.

- **Bit Flip Mutation**

We pick one or more random bits and flip them. For binary encoding GAs, this is used as shown in Figure **I.8.**

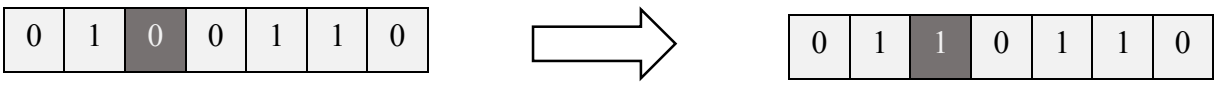

Figure I.8 : Example of Bit Flip Mutation

- **Random Resetting**

Random resetting is a bit twist extension for the integer representation. A random value is assigned to the randomly selected gene from the list of allowable values.

- **Swap Mutation**

We pick two locations on the chromosome on a random basis and switch the values. This is popular in encodings that are on permutation as shown in Figure **I.9**.

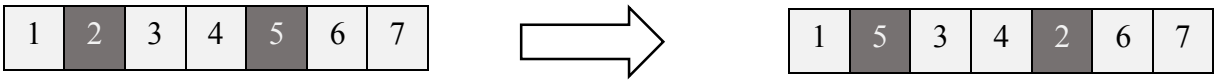

Figure I.9 : Example of swap mutation

- **Scramble Mutation**

Often common with permutation representations, a group of genes is picked from the whole genome and their values are conveniently scrambled or shuffled as shown in Figure **I.10**.

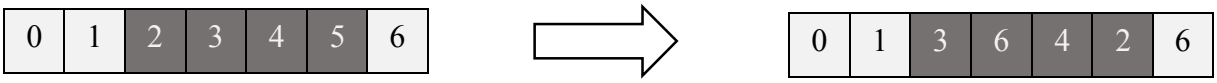

Figure I.10 : Example of scramble mutation

- **Inversion Mutation**

We pick a gene subset like in scramble mutation, and then we merely invert the entire string in the subset instead of shuffling the subset as shown in Figure **I.11**.

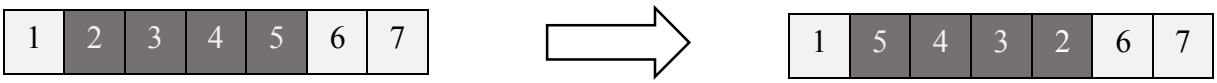

Figure I.11 : Example of Inversion mutation

I.2.1.6 Survivor Selection

The selection plan for survivors defines which individuals must be booted out and which one must be retained in the next generation. It is important to ensure that the fittest individuals are not taken out of the population and that diversity is preserved among the population at the same time.

These GA's are using elitism. Simply put, it means that the current fittest member is always transferred to the next generation. Therefore, the fittest member of the existing population cannot be substituted under any conditions.

Kicking random members out is the easiest policy, yet, this frequently has convergence problems, thus the other strategies are widely used such as Age Based Selection and Fitness Based Selection [23].

I.2.1.7 Termination Condition

The main evolutionary loop stops when the termination condition is established. Often, the genetic algorithm functions for a number of generations defined earlier. For different experimental settings, this can be reasonable. The duration of the optimization process may be limited by the time and cost of fitness function assessment. The convergence of the optimization process is another important termination condition. The advancement of fitness function may decrease considerably when approximating the optimum, although when so significant process is observed, the evolutionary process stops [23].

I.3 Other evolutionary algorithms

I.3.1 Evolution strategy

In 1968, Evolution strategy was introduced in [24]. The genetic algorithm is even newer. The first use of evolution strategy by Schwefel and Klockgether was to allow some experimental optimizations in the flow of air. They noticed that evolution strategy was stronger than other discrete gradient-approaches which raised the interest of people in evolution strategy. The evolution strategy derived less motivation from nature than the previous evolutionary algorithms. It was instead created artificially as a numerical method for optimization. The form of evolution strategy is therefore very distinct from other evolutionary algorithms. For example, evolution strategy scholars call the mutation step size and probability endogenous parameters encoded in the genome of an individual. Thus, besides the gene values, a genome is also composed of the parameter settings that control the convergence progress of the whole algorithm. The notation of evolution strategy is quite interesting. $(\mu / \rho^{+}, \lambda)$ - ES denotes an evolution strategy where μ denotes parent population size; ρ denotes breeding size;$(\mu / \rho + \lambda)$ - ES denotes the algorithm is overlapping; $(\mu / \rho , \lambda)$ denotes that algorithm is not overlapping; and λ denotes the offspring population size [25].

I.3.2 Evolutionary programming

For the learning problem, Fogel used EP to solve it, and in order to present a chromosome he used a finite state machine, which causes some difficulties resolving problems with optimization of EP. In the 90s, several researchers turned EP into an area of optimization and developed various types of EP. The most cited EP is listed as the following solution process, which uses real numbers to represent variables. Algorithm **2** is able to describe the Basic Evolutionary Programming Algorithm **[25]**.

Hence, the implementation of EP listed above can be considered as a (μ +μ)-ES without crossover.

Algorithm 2 Basic Evolutionary Programming Algorithm.

Phase 1: Initialization.

Step 1.1: Assign the parameters for EP, such as λ, μ, and σ.

Step 1.2: Generate μ uniformly distributed individuals randomly to form the initial population and evaluate their fitness values. gen = 0.

Phase 2: Main loop. Repeat the following steps until gen > maxgen.

Step 2.1: Repeat the following operations until a new population with μ individuals has been generated. Perform a mutation for every gene of the individual to generate a new one.

Step 2.2: Calculate the fitness value for every new individual.

Step 2.3: Combine μ current and μ new individuals and pick the μ best ones to form a new population. gen = gen + 1.

Phase 3: Submitting the final μ individuals as the results of EP.

I.3.3 Genetic programming

In 1992, Koza suggested Genetic Programming GP as a tool for computers to solve problems in an automatic way **[26]**. Computer programs are generated automatically by genetic operators, and that is the intuitive idea of GP.

GAs are usually confronted with optimization problem. We must look for optimal variables values in order to achieve a maximum/minimum value for their objective function.

This type of problem is called optimization of parameters, i.e. to find the best parameters of problem [25].

Nevertheless, problems are sometimes more complex. In addition to optimizing the parameters we also face structure optimization. While constructing an artificial neural network, in addition to the determination of the thresholds for each nerve cell, the number of the internal levels nerve cells must be determined as well. We would like to see the optimal parameters of the filter as well as decide the order of the filter as a design of a digital filter system. In general, such design problems have a basic structural optimization prerequisite. However, traditional GAs cannot handle the structures, i.e. GAs cannot express the solution structure in chromosomes.

The above discussion comes from the operations research community, i.e., mathematics point of view. Let us discuss the difference between GP and GAs from the viewpoint of artificial intelligence, i.e., computer science point of view. The requirement is to set up a nonlinear relationship between the input and the output so that this relationship can map correctly the input data to the output data. If so, we say that the relationship has some "intelligence." In the future, if new data come, we can hope that this intelligent relationship would suggest the correct output, that is a forecast, classification, pattern recognition, clustering, etc. learning problem is the name of this kind of nonlinear relationship setup problem, and data mining or knowledge discovery is the name of the research field. While GP can handle learning problems directly, we also can transform them into optimization problems and use GAs to solve them [25].

I.3.4 Swarm intelligence

Swarm intelligence (SI) is a special class of evolutionary algorithm such as Ant Colony Optimization, Particle Swarm Optimization, and Bee Colony Optimization, etc., fall under it. Instead of involving any selection (i.e. birth and death), it maintains a fixed size population of individuals for search across generations. Findings reported by individuals after each generation are recorded and used to adjust the search strategy in the next generation.

Some algorithms are designed originally to find the shortest path. Nevertheless, they have been further generalized for other applications. For example: Bi-Criterion Optimization, Load Balancing in Telecommunication Network, signal processing, image processing, and Power System.

I.4 Conclusion

In this chapter we present an overall of the basics of the Evolutionary Algorithms, we introduce the fundamental concepts and terms associated with the Algorithms. This chapter can serve as a starting point for our thesis objective.

CHAPTER II

Noise Removal and Restoration

II.1 Introduction

There has been a lot of research in image processing in recent years about image denoising [27]. One of the most important subjects in the field of image processing is the elimination of noise from images. to find the closest image to the original noiseless one [28]. This pre-process preserves edges, texture and other information, which is one of its main tasks [29]. In other words, image denoising success affects segmentation, classification and related processes success rate [30], [31]. The purpose of this chapter is to provide a summary of the literature about denoising techniques.

II.2 Literature review

Image denoising has been one of the main issues of image processing in recent years. Several strategies for image denoising in literature have been developed, yet it remains a difficult problem, as many researchers are still studying it. The success of segmentation and classification and comparable actions [32]–[36], is affected by the success of image noise reduction.

Digital images can be prone to a distortion induced by a number of factors, such as image sensor limits, lens imperfections, compression artifacts and transmitting procedures. The problem known as picture denoising addresses these problems with the goal of reducing noise levels and maintaining key characteristics such as corners, edges and texture [37]–[39].

II.2.1 Satellite images

A procedure was suggested in [40] using matched bi-orthogonal wavelets to denoise satellite images and medical images that were distorted with Gaussian additive white noise. According to this method, the noisy image is decomposed using decomposition filters into sub-bands by implementing four levels of wavelet decomposition. Eventually, by using reconstruction filters, the final restructured picture is produced. The next approach proposed by [41] is used for the de-correlation, the improving and the compression of noisy satellite images. In order to accomplish the necessary process with adaptive learning and a fair convergence rate, one key component research method based on neural networks is employed. It is presented in [42], and focuses on the elimination of multiplicative noise from aerial images. The authors reported a model that outperformed the Aubert and Aujol (AA model) for multiplicative noise and edge preservation in terms of signal-to-noise ratio (SNR) and edge preservation index (EPI) [43]. This reported model is based on partial differential equations (PDE).

II.2.2 Medical images

A technique to denoise medical pictures contaminated with gaussian noise was proposed in [44] aiming for a better image quality for better and correct diagnosis. Three alternative approaches were proposed: hybrid cross-median filter, hybrid min-filter and hybrid for noise reduction. Experiments show that the max-filter combination beats various existing methods. The next procedure is proposed in [45] to denoise medical ultrasound and magnetic resonance imaging by preventing Rician and speckle noise using the concept of wavelets. The underlying idea behind this process is to approximate the probabilities and probability density function empirically. The authors argue that this approach is less cumbersome and adapts to unidentified forms of noise. A method to denoise magnetic resonance images from white gaussian noise is presented by [46]. The approach provided in this case for the reconstruction of images utilizes a bilateral filter in the un-decimated wavelet domain. Coefficients of approximation are calculated by the application of an undecimated wavelet on a noisy image. A bilateral filter is then used on these coefficients to denoise and maintain the edges. The image then is replicated with denoised coefficients. The [47] approach uses threshold-based neural networks for

denoising images of breast cancer tumors. This approach works in two stages: image denoising is used to give a better quality of the image and the segmentation is used to isolate the area of interest. Wavelets for efficient detection and denoising for medical images are combined in terms of thresholds with neural networks. The solution presented in [48] addresses a Gaussian noise removal hybrid filter from X-rays, ultrasound and telescopic images. A combination of wavelets and a bilateral filter is the basis of the developed hybrid filter. Applying the bilateral filter before and after the wavelet decomposition generates better results than state-of-the-art algorithms. The efficiency of the proposed hybrid filter [43] was measured by using the image-quality parameters, peak signal-to-noise ratio (PSNR) and image quality index (IQI).

II.2.3 General images

Noise might be caused to digital images by the different sensors that obtain these images. Salt and pepper noise is one of the most common types of noises that may be caused either by bit errors or faulty sensors. During the image denoising process, the main goal to retrieve the original image contaminated by impulse noise or additive noise while preserving the edge details of an image such as corners and textures [49]–[52]. Digital images from [52]–[58] involve linear/non-linear filters. Generally, the most commonly used filters are the non-linear ones because of their superior performance compared to linear filters [59]. The Median Filter (MF) and its derivatives are still a reference in image filtering. The MF filter uses a fixed Window Size (WS) and is applied to all pixels, whereas it is best to use only to noisy pixels [51]. MF suffers from two major problems despite its low-density noise and efficiency, these problems are the blurring of image details and removing thin edges especially in high-density noise [50]. To solve this problem, many filters have been proposed, as an example: Adaptive Median Filter (AMF), which uses an adaptive WS rather than a fixed one. However, despite the good performance in high-density SPN compared with other noise removal methods, if the WS is large, it prevents finding the pixel that corresponds to the pixel of the original image [60]. The Decision-Based Algorithm (DBA) is derived from MF, it processes only the noisy pixels [61]. In high-density SPN, Modified Decision-Based Unsymmetrical Trimmed Median filter (MDBUTMF) is used. An adaptive window is used to determine and remove the noisy pixels, then MF is applied to them [62]. Noise Adaptive Fuzzy Switching Median Filter (NAFSM) uses the histogram to detect noise pixels of contaminated images. The noise pixels are replaced using an MF or estimated according to their neighbors' values [14]. In Based on Pixel Density Filter (BPDF), the noisy pixel is replaced by the most repetitive pixel value in the adaptive window among the noiseless neighboring values [63]. The proposed Different Applied Median

Filter (DAMF) is the most successful method when the Noise Density (ND) is high. This method uses an adaptive WS and the values of neighbor pixels to approach the original pixel value, and then to acquire the approximate values for the remaining noisy pixels from the first stage [64]. Recently, one of the most efficient methods of removing high-level SPN is an Adaptive Weighted Mean Filter (AWMF). For every pixel, it continuously chooses the adaptive WS by constantly expanding WS in order to acquire equal maximum and minimum values of two consecutive windows. The next step is: if the specified pixel value is the same as the maximum or the minimum values, it would be replaced by the weighted average and that is in the ongoing window, otherwise it would not be adjusted [16].

II.3 Noise Models

Several factors namely movement when capturing the image, limitation in the size of the sensors, imperfections of the camera lens, etc., can often cause a degradation process of the digital image. These situations along with problems that can occur during image compression and transmission can produce a noisy or out-of-focus image, as Figures II.1 and II.2 shows.

Figure II.1 : Example of Noisy image

Figure II.2 : Example of Blurry image

- **Impulsive noise:** Defined by Equation (2.1). Also called salt-and-pepper noise; if b> a, intensity "b" would be a bright spot in the image and "a" dark spot, as long as Pa and Pb are not equal to zero. Usually, in a model where the pixel values are in the range [0. 255], Pa = 0 and Pb = 255

$$p(z)=\begin{cases} p_a & z=a \\ p_b & z=b \\ 0 & other\ case \end{cases} \tag{2.1}$$

- **Rayleigh Noise:** Defined by equation (2.2), where a is a real value and b is a real greater than zero

$$p(z)=\begin{cases} \frac{2}{a}(z-a)e^{-\frac{(z-a)^2}{b}} & z\geq a \\ 0 & z<a \end{cases} \tag{2.2}$$

- **Erlang Noise:** Defined by equation (2.3), where a is a real greater than zero and b a positive integer

$$p(z)=\begin{cases} \frac{a^b z^{b-1}}{(b-1)!}e^{-az} & z\geq a \\ 0 & z<a \end{cases} \tag{2.3}$$

- **Exponential noise:** Defined by Equation (2.4). This is a specific case of Erlang noise for b = 1

$$p(z) = \begin{cases} a\, e^{-az} & z \geq a \\ 0 & z < a \end{cases} \tag{2.4}$$

- **Uniform noise:** Defined by Equation (2.5)

$$p(z) = \begin{cases} \frac{1}{b-a} & a \leq z \leq b \\ 0 & other\ cases \end{cases} \tag{2.5}$$

- **Gaussian noise:** Defined by equation (2.6), where z is the shade of gray, $\bar{z}$ is the mean and σ is the standard deviation.

$$p(z) = \frac{1}{\sigma\sqrt{2\pi}} e^{\frac{(z-\bar{z})^2}{2\sigma^2}} \tag{2.6}$$

Figure II.3 shows an example of when the effect of each of these noises is applied to an image in Figure II.4.

Salt and pepper noise is a type of noise that is the most used in literature due to its ease of handling, hence it is used in this work as well.

II.4 Image denoising by minimizing total variation

A particularly effective and well-used way of suppressing noise in images is to minimize the total variation present in the image. In this way, a mathematical model TV-L2 mode that describes this variation can be used as a guide for several optimization methods [65]. Based on this, a model was proposed in [66] in order to minimize this total variation through the following equation (2.7).

$$min_X \left\{ |\nabla X| + \int_\Omega \frac{\lambda}{2} |X - I|^2 \right\} \tag{2.7}$$

where the first term is the total variation of X, the second term is the data fidelity term, and $\lambda > 0$ is a constant parameter that balances the contributions of the smooth term and the data fitting term. In this proposal, X is the evaluated image and I is the noisy image, ∇X is the gradient of X (full variation norm) and Ω is the set of image points.

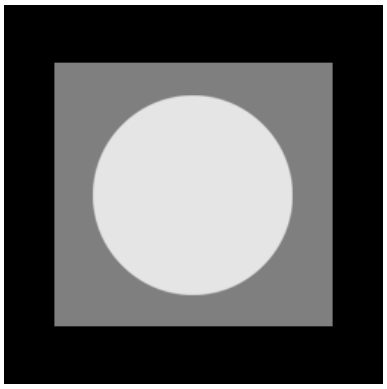

Figure II.3 : Test image

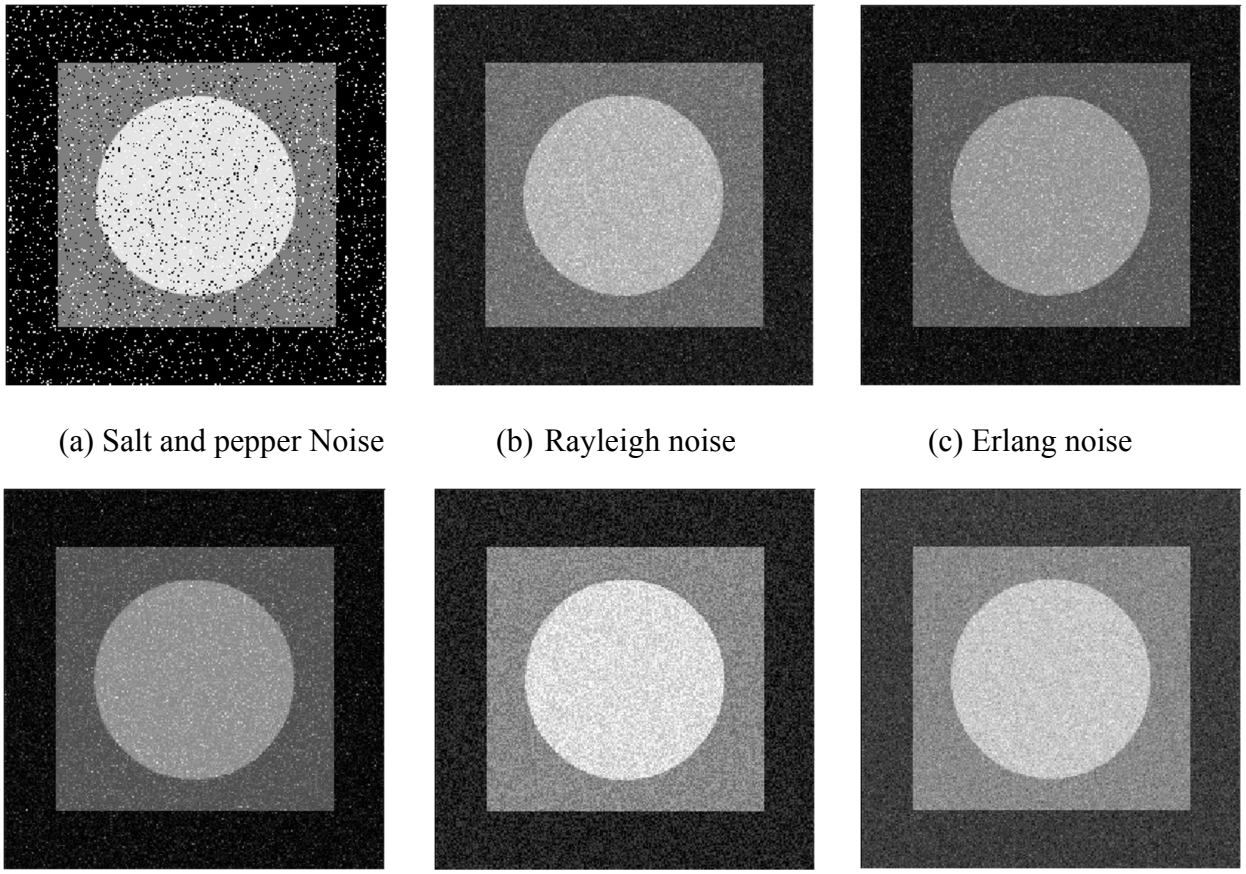

(a) Salt and pepper Noise (b) Rayleigh noise (c) Erlang noise

(d) Exponential noise (e) uniform noise (f) Gaussien Noise

Figure II.4 : The result of different noises applied to Test image

From Equation (**2.7**), different proposals were made, seeking to make the minimization function aware of important image characteristics, such as borders, and more adaptable within space. For this reason, the norm of total variation is now also weighted by a parameter β in equation (**2.8**) **[67]**.

For the development of the work presented in **[65]**, the Beltrami Framework is used. This geometric framework, presented in **[67]**, is based on the concept of action by Polyakov, initially

introduced in string theory in the field of physics. The framework consists of two main aspects: first, describing an image as maps between two varieties of Riemann; second, a functional action that allows measurements in the spaces of these maps.

From the possibilities produced by the use of this framework, Zosso and Bustin proposed a formulation in a primal-dual model of the function described in Equation (**2.8**)

$$min_X \left\{ \int_\Omega \sqrt{1+\beta^2|\nabla X|^2} \quad + \int_\Omega \frac{\lambda}{2}|X-I|^2 \right\} \tag{2.8}$$

The TV-L2 model is very good for removing Gaussian noise, but it is not suitable to remove non-Gaussian noise. It has been shown in **[68]** that minimizing the L1 norm of the difference the between the observed and reconstructed images is more appropriate than minimizing its L2 norm. The TV-L1 model in **[68]** described in Equation (**2.9**) reads as follows:

$$min_X \left\{ |\nabla X| + \int_\Omega \lambda|X-I| \quad \right\} \tag{2.9}$$

where $\lambda > 0$ is a weighted parameter usually chosen by trial and error method according to tested images. In **[69]**, the authors observed that the TV-L1 model is ‘‘more geometric’’ in the sense that it makes faster disappearance of the small shapes, such as salt and pepper noise, than image features with lower contrast. Moreover, the l_1 data fitting leads to a sparse solution that forces the error free reconstruction at many pixels, but allows a relatively large error in the certain number of pixels. This is good for removing salt and pepper noise, since the reconstruction error at the noisy pixels should not be very small. However, the TV-L1 model can destroy the uncontaminated intensities especially when the noise level is high because of the difficulty in distinguishing fine structures from the noises **[68]**.

After studying, we suggest a new function drawn from Equation (**2.8**) and (**2.9**).

$$min_X \left\{ \int_\Omega \sqrt{1+\beta^2|\nabla X|^2} \quad + \int_\Omega \lambda|X-I| \quad \right\} \tag{2.10}$$

where $\lambda > 0$ and $1 \geq \beta \geq 2$ are balancing parameters usually chosen by trial and error method according to tested images, used in this work, in its discrete form, as the EHGA fitness function. Through a projected gradient optimization algorithm, they were able to achieve better results than using the function originally proposed in **[68]**.

II.5 Image denoising based on optimization algorithm

The problem of denoising, one example of such an approach is presented in [70], where image denoising takes place through the application of particle swarm optimization (PSO) combined with non-local mean filtering. The non-local mean filter's parameters are calculated by a PSO algorithm and the collected images are evaluated by a metric Q every time. This metric shows a measure of the true content of the image as described in [70]. The approach refines the non-local mean filter parameters until an optimal solution is found or the highest number of iterations is obtained. The algorithm of artificial bee colony, presented by Kockanat [71], is another example of a metaheuristic approach to image denoising. The algorithm is driven by a Mean Squared Error (MSE). By calculating the noisy signal and extracting it from the input image where an estimated ideal image is defined, the MSE is calculated between it and an image under evaluation. In the literature, dealing with noisy images has also different evolutionary approaches. Some of these approaches are used to approximate the thresholds to perform wavelet shrinkage, as defined in [72], which used a Differential Evolution Strategy. The authors in [73] find threshold values using a Multi-Objective Genetic Algorithm. A genetic algorithm is proposed by [39] to perform image denoising, where the images are individuals and a population evolves applying tailor-made crossover and mutation operators. Crossover operators by exchanging pieces of images create new individuals, while the mutation operators are simple filters such as averaging filters, median filters and Gaussian filters applied over the images. HGA is similar to the method used in [39] when a noisy image is used as input and mutation is applied this to input initialize a population. In fact, [39] introduced two of the three crossover operators present in the HGA. However, HGA not only offers another genetic algorithm, but also employs a different fitness function for the guidance of the evolution, and uses as local search operators, some of the most important image denoising methods in the literature. This work expands the previous results published in [38], where parameter assessments are stated as well as some comparisons with just few images.

Algorithm in image restoration are [37], [74]–[76]. A hybrid genetic algorithm is used in [37] for the purpose of eliminating the added Gaussian density in grey images that integrates some of the best filters with the features of a GA in order to improve the image. In [76], a HGA that aims to eliminate the impulsive noise in color images integrates as primary solutions the output images of adaptive and robust filters.

II.6 Conclusion

Good quality amount of research has been done in the field of image denoising for digital images, but during the review of the literature, we identified the following research gaps.

Despite this interest, there exist no genetic algorithms intended to remove SPN in grey images by evolving images.

Improve the medical image contaminated with SPN.

Improve the original image contaminated with SPN while preserving image edge details, such as texture and corners.

CHAPTER III

Effective Hybrid Genetic Algorithm-proposed algorithm-

III.1 Introduction

The proposed algorithm presented in this work is a genetic algorithm for noise suppression in images. In this approach, we can highlight that each individual in the population is an image itself, represented by an array of pixels whose values are integers ranging from 0 to 255.

This chapter has two main parts. In the first part, the steps of the proposed algorithm from the noisy image that we considered as an input are applied and then comes the creation of the initial population. Finally, the steps of the genetic algorithm from selection, crossover, mutation until the denoised image is obtained.

The other section highlights metrics to measure the quality of images. The examples are taken into account to explore the quality of the filtered image with the EHGA method.

III.2 Preliminaries and EHGA Algorithm

The implementation of the effective hybrid genetic algorithm follows the following procedure step

Algorithm 3 Effective hybrid genetic algorithm (Proposed algorithm)

Step 1 Input image *I (i, j)*

Read a noisy image is represented by an array of pixels *I (i, j)* where *i* and *j* range from 0 to 255 and 255, respectively.

Step 2 Initialization of the initial population:

To set the initial population, create a group of three individuals D= {I_{DAMF}, I_{AWMF}, I_{FNAFSM}} by executing filters DAMF, AWMF and NAFSM over image *I (i, j)*. After that, in order for the initial population to reach N_p individuals, apply a pixel combination between a random selection of two individuals from set D and keep combining the results until the initial population reaches N_p individuals.

Step 3 Evaluation of initial population:

Evaluate the fitness of the initial population.

Step 4 Create new individuals:

1- Use a roulette wheel selection to select a pair of initial individuals.
2- The new individuals are created by crossing over this pair by randomly executing one out of the four crossover operators.
3- Apply randomly one of the four mutation operations to mutate each new individual with probability N_m until the new population reaches $N_c \times N_p$ individuals.

Step 5 Evaluation of new population:

Evaluate the fitness of new initial individuals.

Step 6 Update the initial population:

The population (initial population and new population) is sorted based on the values of their fitness with recording the best N_p individuals, these individuals will be retained for the next iteration as an initial population.

Step 7 Check termination criterion:

Repeat steps 4 to 6 until $Iter_{max}$ is reached. The denoised image *F(i, j)* is the individual with the best fitness value in the last generation.

More details concerning the proposed algorithm are depicted as follows

III.2.1 Initialization

The second step of the algorithm is to create an initial population of images after two phases, the first one is when the three filters {DAMF, AWMF, NAFSM} are applied over a noisy image and then include the results of these methods in the initial population.

Second, the rest of the initial population is created by randomly selecting two of the first step outputs. Then, a pixel recombination procedure that randomly selects pixel by pixel is applied between the two selected outputs.

This process produces a new individual that is introduced into the initial population until the it reaches N_p individuals. All of the initial population represents an improved version of input image *I(i, j)*. Figure **III.1** illustrates an initialization of the EHGA population.

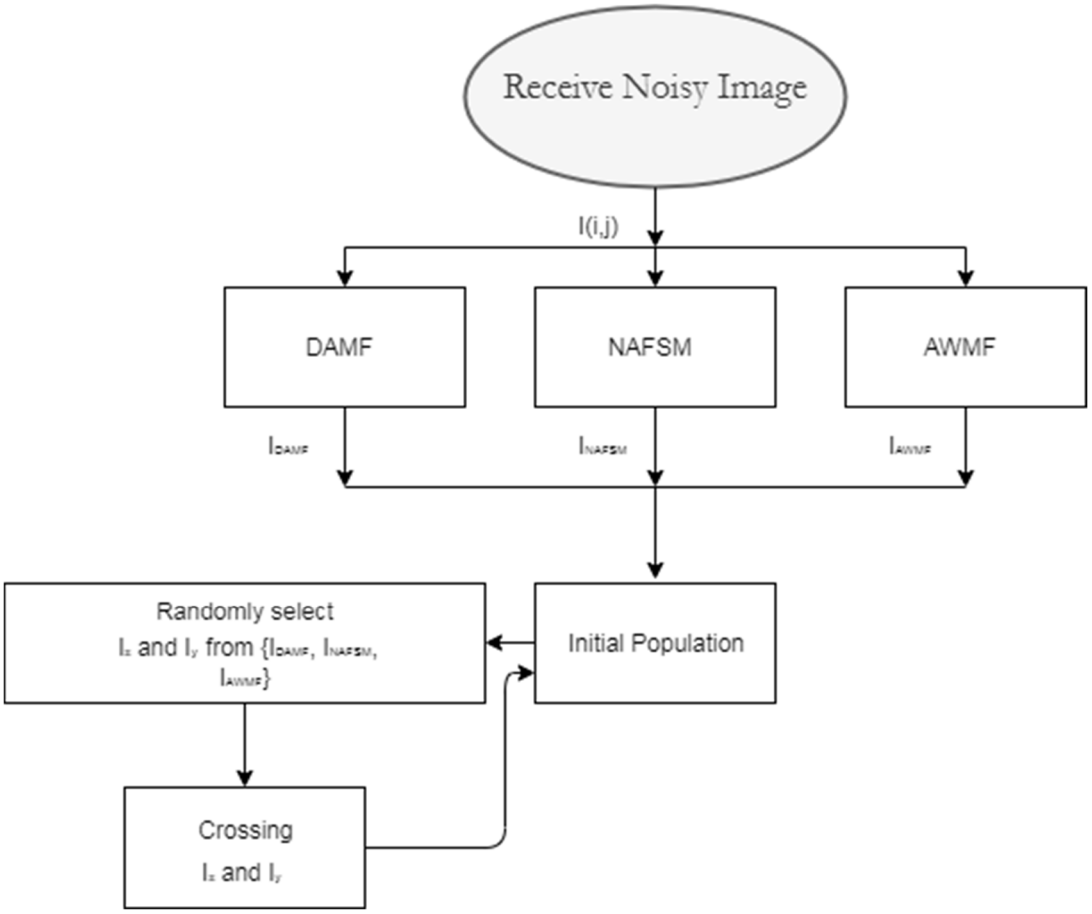

Figure III.1 : Initialization of the EHGA population.

III.2.2 Fitness Evaluation

In steps 3 and 5 of this algorithm, an evaluation of the created individuals is done using a fitness function that selects the best individual among the created ones. The fitness function is given by:

$$fitness(F) = \lambda|F - I| + \left(\sum_{\Omega} \sqrt{1 + \beta^2 |\nabla F|^2}\right) \quad (3.1)$$

This function preserves important features of the image such as edges and corners. The fitness function stems from [77][65]. The object is to minimize equation (3.1) where Ω is the group of all points in the image, the parameter ∇F is a Total Variation (TV) regularizing term, β and λ are balancing parameters. The term $|F - I|$ is called fidelity term, which ensures a certain degree of fidelity between the original image and the image being evaluated, where F is the image being evaluated, which is an approximation of the original image and I is the noisy image. We are essentially trying to reduce the regularizing term of the recovered image while preserving the fidelity term relevant to the original image [65][78].

III.2.3 Parent Selection

In Step 4.1 of the proposed algorithm, select a pair of initial individuals by Roulette Wheel selection.

III.2.4 Crossovers

In Step 4.2 of the proposed algorithm, apply crossover operations where four crossovers are used by randomly selecting one of them Figures III.2 - III.7 illustrates a result of this crossover.

III.2.4.1 Single-point:

Single-point: a point on both parents is selected by a single crossover, and during this process, one of the two is haphazardly chosen. as shown in Figures III.2 and III.3.

- ***One-point column***: first, a column of pixels is selected randomly and then, from one parent, all the pixels at the top of this column, and from the other parent, all the pixels under that column. [37], [39]. Figure III.2**.**

- ***One-point row*****:** the same as the previous method, yet herein a column is selected instead of a row. [37], [39] as shown in Figure III.3**.**

(a) Parent 1 (b) Parent 2 (c) Child

Figure III.2 : Example of One-point column crossover.

(a) Parent 1 (b) Parent 2 (c) Child

Figure III.3 : Example of One-point row crossover.

III.2.4.2 Two-point:

A two-point crossover selects two points on both parents. In this process, one of the two is randomly chosen.

- ***Two-point column*:** two points are selected randomly from the column; all pixels are copied from the beginning of the chromosome to the first crossover point from a first parent. Then, all the pixels are copied from the first to the second crossover point from a second parent and the rest is copied from the first parent [78]. as shown in Figure III.4**.**

(a) Parent 1 (b) Parent 2 (c) Child

Figure III.4 : Example of Two-point column crossover.

- ***Two-point row*:** the same as the previous method taking into account the selection of a row instead of a column [78]. as shown in Figure III.5**.**

(a) Parent 1 (b) Parent 2 (c) Child

Figure III.5 : Example of Two-point row crossover.

III.2.4.3 Cross Grid:

A mixture between One-point column and One-point row operators is used, where the image is divided into four parts, then one part of each pair of images is exchanged (the parts are not necessarily equal in size)[79] as shown in Figure III.6**.**

(a) Parent 1 (b) Parent 2 (c) Child

Figure III.6 : Example of Cross Grid crossover.

III.2.4.4 Pixel-by-pixel random:

Random selection of each pixel from one parent creates a new individual [78] as shown in Figure III.7.

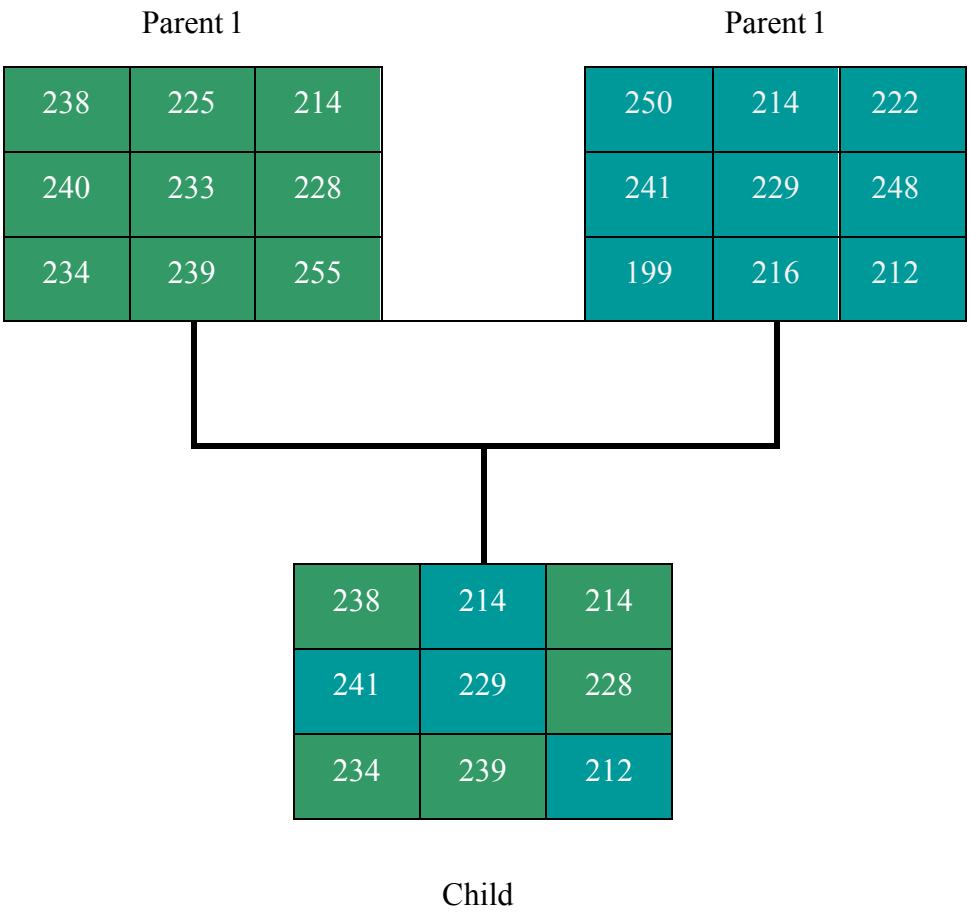

Figure III.7 : Example of Pixel-by-pixel random crossover.

III.2.5 Mutation

Thirdly, the mutation operations are performed on the new individual through one of the four mutations applied, which are also randomly selected.

- NAFSM [14]
- DAMF [15]
- AWMF [16]
- Random: each pixel of an individual is multiplied by a random value from the interval [0.8, 1.2], while preserving the noise-free pixel of $X(i, j)$ unchanged [78].

III.2.6 Update the initial population:

A new population from the union of some individuals of the previous generation and some of their offspring's is generated by line 12 of Algorithm 3. To select such individuals, a fitness-based replacement scheme is used, this latter introduces elitism into the evolutionary process and guarantees the survival of the fittest individual.

III.2.7 Check termination criterion

The algorithm is iterated until it reaches $Iter_{max}$ by line 13 of Algorithm **3**, then the best individual found in the last generation is returned (see line 14).

Figure **III.8**, illustrates the basic flowchart of EHGA

III.3 Metrics to Measure the Quality of Images

We use the six image quality metrics that are commonly used in literature. Peak Signal to Noise Ratio (PSNR), Structural Similarity Index (SSIM), Image Enhancement Factor (IEF), Universal Quality Index (UQI), Visual Information Fidelity (VIF) and Mean Structural Similarity (MSSIM). to measure the quality of output images after a filtering process by using test images.

These metrics provide quantitative values of how close or far the output images are from an original reference image (commonly without noise).

III.3.1 Peak signal to noise ratio

Peak Signal to Noise Ratio (PSNR), which is the most used in literature, is defined as:

$$PSNR_{dB} = 10 \cdot log\left(\frac{255^2}{MSE}\right) \tag{3.2}$$

where MSE (Mean Square Error) is defined as:

$$MSE = \frac{1}{M \times N}\sum_{i=0}^{M-1}\sum_{j=0}^{N-1}[O(i,j) - F(i,j)]^2 \tag{3.3}$$

where *O(i, j)* and *F(i, j)* are the original and the denoised images, respectively. Where *M* and *N* are the image dimensions.

III.3.2 Structural similarity index metric

Structural Similarity Index Metric (SSIM), which can be mathematically formulated **[80]**, is defined as:

$$SSIM(A,B) = \frac{(2\mu_A\mu_B + c_1)(2\sigma_{AB} + c_2)}{(\mu_A^2 + \mu_B^2 + c_1)(\sigma_A^2 + \sigma_B^2 + c_2)} \tag{3.4}$$

where $\mu_A,\ \mu_B, \sigma_A^2,\ \sigma_B^2, and\ \sigma_{AB}$ are the mean intensities, standard deviations and covariance for images A and B, respectively. $c_1 = (k_1 L)^2$and $c_2 = (k_2 L)^2$ that $L = 255$ for 8-bit grayscale images and k_1=0.01 and k_2=0.03 are constant

III.3.3 Image enhancement factor

Image Enhancement Factor(IEF), which is given in [62], is simplified as :

$$IEF = \frac{\sum_{i=0}^{M-1}\sum_{j=0}^{N-1}[X(i,j)-O(i,j)]^2}{\sum_{i=0}^{M-1}\sum_{j=0}^{N-1}[F(i,j)-O(i,j)]^2} \tag{3.5}$$

where *O(i,j)* is the original image, *F(i,j)* is the denoised image, and *X(i,j)* is the noise image, *M* and *N* are the dimensions of the image.

III.3.4 Universal quality index

This matric is easy to calculate and applicable to various image processing applications. Instead of using traditional error summation methods, the proposed index is designed by modeling any image distortion as a combination of three factors: loss of correlation, luminance distortion, and contrast distortion. Although the new index is mathematically defined and no human visual system model is explicitly employed, our experiments on various image distortion types indicate that it performs significantly better than the widely used distortion metric mean squared error [81].

UQI (Universal Quality Index), which is given in [81], is defined as:

$$UQI = \frac{4m_O m_F \sigma_{OF}}{(m_O^2+m_F^2)(\sigma_O^2+\sigma_F^2)} \tag{3.6}$$

Where

$$m_0 = \frac{1}{M\times N}\sum_{i=0}^{M-1}\sum_{j=0}^{N-1} O(i,j) \tag{3.7}$$

$$m_F = \frac{1}{M\times N}\sum_{i=0}^{M-1}\sum_{j=0}^{N-1} F(i,j) \tag{3.8}$$

$$\sigma_F = \frac{1}{(M\times N)}\sum_{i=0}^{M-1}\sum_{j=0}^{N-1} [F(i,j)-m_F]^2 \tag{3.9}$$

$$\sigma_O = \frac{1}{(M\times N)}\sum_{i=0}^{M-1}\sum_{j=0}^{N-1} [O(i,j)-m_O]^2 \tag{3.10}$$

$$\sigma_{OF} = \frac{1}{(M\times N)-1}\sum_{i=0}^{M-1}\sum_{j=0}^{N-1} [O(i,j)-m_O][F(i,j)-m_F] \tag{3.11}$$

where M and N are the image dimensions, *O(i,j)* is the original image and *F(i,j)* is the denoised image.

III.3.5 Visual Information Fidelity

Visual Information Fidelity (VIF) is an image information measure that quantifies the information that is present in the reference image, and also quantifies how much of this reference information can be extracted from the distorted image. Ii is defined in **[82]**.

$$VIF(U,V) = \frac{\sum_{j\epsilon subbands} I(\vec{C}^{N,j};\vec{F}^{N,j}|s^{N,j})}{\sum_{j\epsilon subbands} I(\vec{C}^{N,j};\vec{E}^{N,j}|s^{N,j})} \tag{3.12}$$

Where

$$I\left(\vec{C}^{N,j};\vec{E}^{N,j}\middle|s^{N,j}\right) = \frac{1}{2}\sum_{i=1}^{N}\sum_{k=1}^{M}\log\left(1+\frac{s_i^2\lambda_k}{\sigma_n^2}\right) \tag{3.13}$$

$$I\left(\vec{C}^{N,j};\vec{F}^{N,j}\middle|s^{N,j}\right) = \frac{1}{2}\sum_{i=1}^{N}\sum_{k=1}^{M}\log\left(1+\frac{g^2 s_i^2\lambda_k}{\sigma_u^2+\sigma_n^2}\right) \tag{3.14}$$

Where

$I\left(\vec{C}^{N,j};\vec{E}^{N,j}\middle|s^{N,j}\right)$ and $I\left(\vec{C}^{N,j};\vec{F}^{N,j}\middle|s^{N,j}\right)$ represent the information that can ideally be extracted by the brain from a particular sub band in the reference and the test images, respectively. For more details, see **[82][83]**.

III.3.6 Mean Structural Similarity

Mean Structural Similarity (MSSIM) which is given in **[84]**, is simplified as :

$$MSSIM(U,V) = (I_m(U,V)^{\alpha M}\prod_{j=1}^{M}(c_j(U,V))^{\beta_j}\times(s_j(U,V))^{\gamma_j} \tag{3.15}$$

Where

$$l_M(U,V) = \frac{2\mu_U\mu_V+C_1}{\mu_U^2+\mu_V^2+C_1} \tag{3.16}$$

on scale M,

$$c_j(U,V) = \frac{2\sigma_U\sigma_V+C_1}{\sigma_U^2+\sigma_V^2+C_2} \tag{3.17}$$

on each scale j = 1, ..,M

$$S_J(U,V) = \frac{\sigma_{UV}+C_3}{\sigma_U\sigma_V+C_3} \tag{3.18}$$

on each scale j = 1, ..,M

$c_1 = (k_1 L)^2$, $c_2 = (k_2 L)^2$ and $c_3 = \frac{c_2}{2}$ that L = 255 for 8-bit grayscale images and k_1=0.01 and k_2=0.03 are constant.

j represents a resolution scale after each low-pass filtering and down sampling, and M represents the total number of scales; *α, βj, γj* are used to adjust the relative importance of different components. In experiments, we use five scales as in **[85]**, i.e., M = 5. MSSIM is better than SSIM in terms of its correlation with a human judgment of images **[85]**.

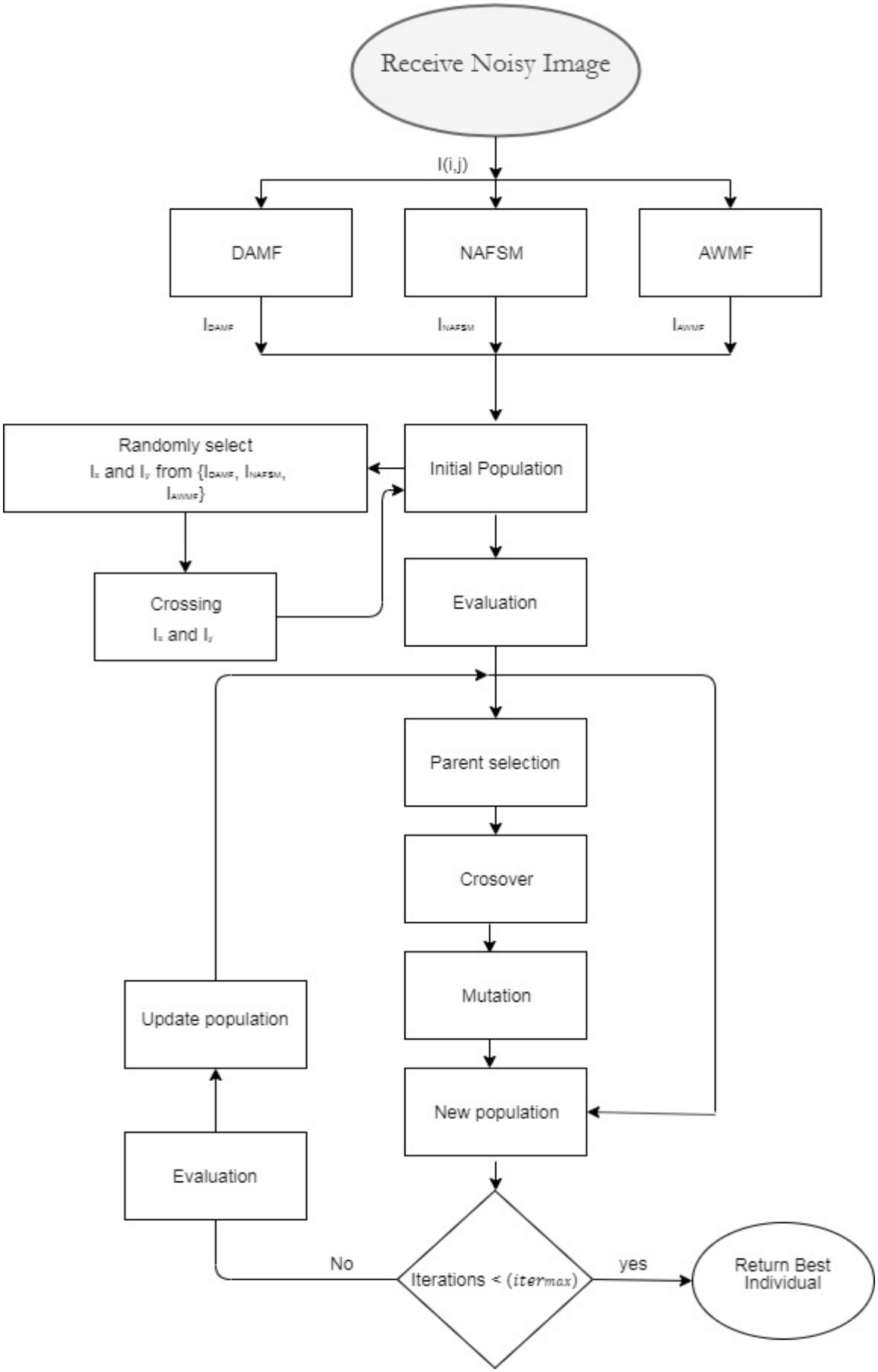

Figure III.8 : Basic flowchart of EHGA operation.

III.4 Conclusion

In the first section, a new genetic algorithm is introduced, called the Effective Hybrid Genetic Algorithm (EHGA). It is an optimization algorithm that relies on combining the genetic algorithm with 3 of the best filters in suppressing the salt and pepper noise to create the initial set and it is also used in mutation. New methods have been created for use in a crossover, along with a new function based on total variation in image denoising.

In the second section, we present the 6 most important metrics to measure the quality of images for use in the next chapter to measure the efficiency of the proposed algorithm against known and recent methods in the last five years.

CHAPTER IV

Applications, results and Discussions

IV.1 Introduction

This chapter presents the computational results obtained by the EHGA. First, materials and methods are presented (section IV.2). Then the images used in the test (Section IV.3). Next, a parameter set of the EHGA (section IV.4). Then the quality of the EHGA is tested against methods in the literature (section IV.5) and with the use of EHGA in medical images (section IV.6).

IV.2 Materials and methods

The algorithms used for experimental results comparison are: Adaptive Median Filter (Hwang and Haddad.1995) **[60]**, Decision Based Algorithm (Pok and Jyh-Charn Liu. 1999) **[86]**, Noise Adaptive Fuzzy Switching Median Filter (Toh and al. 2010) **[14]**, Modified Decision-Based Unsymmetrical Trimmed Median Filter (Esakkirajan and al. 2011) **[62]**, Adaptive Weighted Mean Filter (Zhang and LI. 2014) **[16]**, Different Applied Median Filter (Erkan and al. 2018) **[15]**, Based on Pixel Density Filter (Erkan and Gökrem. 2018) **[87]**, along with the Effective Hybrid Genetic Algorithm (proposed algorithm) **[78]**.

The methods applied in the comparisons and their respective abbreviations used in this work are described in Table **IV.1.**

Table IV.1 : Methods and their respective abbreviations

Methods	Abbreviation
Adaptive Median Filter	AMF
Decision Based Algorithm	DBA
Noise Adaptive Fuzzy Switching Median Filter	NAFSM
Modified Decision-Based Unsymmetrical Trimmed Median Filter	MDBUTMFG
Different Applied Median Filter	DAMF
Adaptive Weighted Mean Filter	AWMF
Based on Pixel Density Filter	BPDF
Effective Hybrid Genetic Algorithm	EHGA

IV.3 Image database

Simulations for all the tests on 16 standard test images are conducted to evaluate the performance comparisons for the different methods. The utilized images are (Baboon, Barbara, Blonde Woman, Boat, Bridge, Cameraman, Couple, Elaine, Flintstones, Hill, Lake, Lenna, Man, Parrot, Peppers and Plane) (Figure **IV.1**), and 30 Test images are obtained from Database (Figure **IV.2**) **[88]**, along with five medical images (Figure **IV.3**)

Figure IV.1 : Standard images

Figure IV.2 : 30 Test images acquired from Database

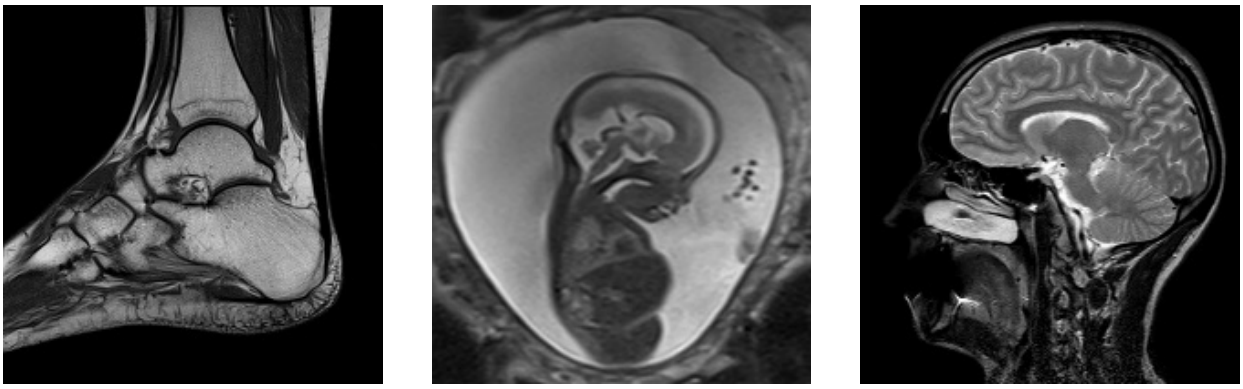

Ankle Fetal Head

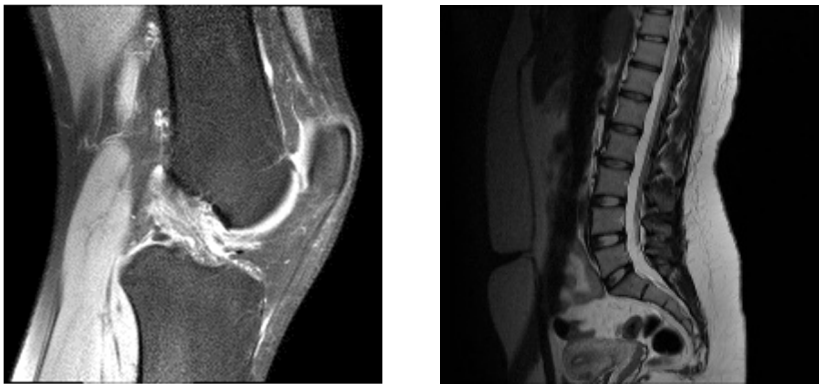

Knee Lumbar

Figure IV.3 : Medical images

IV.4 Configuration set of the algorithm EHGA.

The tests were performed for the purpose of finding an appropriate configuration for EHGA parameters. The different values for a specific parameter are evaluated by each test, after that for each best image obtained, the aforementioned metrics were calculated and the values were compared one against other.

Some empirical tests are the base of this configuration, taking into consideration the time spent for executing the GA combined with the other denoising methods. As an example, initialization, mutation processes are very time-consuming when setting a large-sized population, thus it is not possible to set such a population. Table IV.2 represents the configuration set of the algorithm EHGA.

We selected this configuration set by the execution of preliminary trials considering the tradeoff between time and efficiency

EHGA and the other methods were executed 10 times for each image and for each noise density (ND). We executed the experiments on a 2.0 GHz Intel Core i3-5005, with 4 GB of RAM, and under the operating system Windows 7. The proposed algorithm was coded in MATLAB R2013a.

Table IV.2 : The configuration set of the algorithm EHGA.

Size of the population (N_s)	60
Mutation rate (N_m)	0.02
Completion-criteria ($Iter_{max}$) max iterations	5
Crossover rate (N_c)	0.95
β	1
λ	0.075
Selection criteria	Roulette wheel selection

IV.5 Caparisons EHGA with methods in the literature

The comparison of the other existing methods mentioned in Chapter **II** with the quantitative and visual performance of the EHGA to remove SPN generates experimental results that are demonstrated in this chapter. The simulation test was conducted on 30 test images in Database **[88]** and 16 standard test images with a size of 512 × 512. SPN are used to perturb each one of them with nine different Noise Densities (NDs) (10%, 20% 30%, 50%, 60%, 70%, 80% and 90%). The values highlighted in bold are the best values for that noise level and the values underlined are the worst values.

Table **IV.3** presents the average PSNR, SSIM, IEF, and UQI results for all methods that are mentioned in Chapter **II** for each ND from 10% to 90% for 16 standard images.

Table **IV.4** presents the average PSNR, SSIM, IEF, and UQI results of the methods for 30 test images in the TEST IMAGES Database **[88]**, with NDs from going 10% to 90%.

Based on the results of Tables **IV.3** and **IV.4**, when the noise level is above 40%, the other methods are less effective than the EHGA. In fact, when ND is medium or high, EHGA is the best and most effective method when it is compared to the other methods. The values highlighted in bold are the best values for that noise level and the values underlined are the worst values.

Table IV.3 : Median results of the algorithms for the 16 standard images

Algorithm	Evaluation	10%	20%	30%	40%	50%	60%	70%	80%	90%
AMF	PSNR	22,5870	22,5232	22,4324	22,2456	21,4835	19,2711	15,7208	11,8794	8,3420
	SSIM	0,6830	0,6774	0,6720	0,6626	0,6272	0,5184	0,3144	0,1220	0,0354
	IEF	6	12	17	22	23	16	8	4	2
	UQI	0,7241	0,7190	0,7135	0,6991	0,6303	0,4689	0,2880	0,1497	0,0565
DBA	PSNR	33,7118	30,3239	28,1839	26,5157	25,1299	23,8330	22,4865	20,8349	18,3927
	SSIM	0,9834	0,9615	0,9329	0,8977	0,8569	0,8066	0,7447	0,6580	0,5178
	IEF	74	67	62	57	51	46	39	30	19
	UQI	0,9849	0,9662	0,9422	0,9129	0,8784	0,8354	0,7788	0,6888	0,5114
BPDF	PSNR	36,1478	32,5320	30,0852	27,9445	25,9870	23,8363	21,2621	17,0427	10,0877
	SSIM	0,9789	0,9534	0,9218	0,8815	0,8290	0,7567	0,6537	0,4810	0,2183
	IEF	152	125	105	84	66	48	31	13	3
	UQI	0,9828	0,9621	0,9359	0,9009	0,8532	0,7780	0,6511	0,4020	0,0992
MDBUTMF	PSNR	38,6557	35,1732	32,9494	31,0934	29,1580	26,4570	23,0148	19,1401	15,1895
	SSIM	0,9862	**0,9700**	0,9508	0,9260	0,8861	0,8007	0,6301	0,3911	0,1771
	IEF	293	248	216	185	142	86	43	20	9
	UQI	0,9888	**0,9756**	0,9592	0,9355	0,8819	0,7713	0,6179	0,4402	0,2429
DAMF	PSNR	**38,8641**	**35,2179**	**32,9502**	31,2643	29,8272	28,4453	27,1168	25,5990	23,4147
	SSIM	**0,9864**	**0,9700**	**0,9511**	0,9287	0,9027	0,8709	0,8314	0,7767	0,6851
	IEF	**311**	**249**	**218**	194	172	150	127	101	67
	UQI	**0,9890**	**0,9756**	**0,9601**	0,9418	0,9202	0,8937	0,8601	0,8114	0,7170
NAFSM	PSNR	35,2627	32,2973	30,4754	29,1410	28,0371	26,9699	25,8424	24,5826	21,7578
	SSIM	0,9756	0,9504	0,9239	0,8950	0,8638	0,8275	0,7836	0,7256	0,6025
	IEF	127	125	123	119	115	107	94	78	43
	UQI	0,9776	0,9562	0,9333	0,9084	0,8805	0,8469	0,8026	0,7385	0,5696
AWMF	PSNR	35,2865	33,7856	32,5628	31,4133	30,2478	28,9179	27,4114	25,5496	23,7100
	SSIM	0,9743	0,9627	0,9481	0,9299	0,9076	0,8777	0,8305	0,7608	0,6881
	IEF	123	173	196	201	190	167	140	106	74
	UQI	0,9788	0,9698	0,9580	0,9434	0,9247	0,8999	0,8586	0,7949	0,7231
EHGA	PSNR	38,5701	35,1148	32,6587	**31,4949**	**30,2909**	**28,9903**	**27,5444**	**25,9312**	**23,7614**
	SSIM	0,9862	0,9686	0,9485	**0,9308**	**0,9085**	**0,8792**	**0,8383**	**0,7819**	**0,6913**
	IEF	292	243	201	**206**	**193**	**171**	**142**	**111**	**75**
	UQI	0,9888	0,9748	0,9585	**0,9439**	**0,9256**	**0,9010**	**0,8663**	**0,8163**	**0,7268**

Table IV.4 : Median results of the algorithms for the 30 images for TESTIMAGES gallery

Algorithm	Evaluation	10%	20%	30%	40%	50%	60%	70%	80%	90%
AMF	PSNR	16,3709	16,3403	16,2670	16,1293	15,8392	14,9776	12,9757	10,3873	7,7158
	SSIM	0,5345	0,5322	0,5275	0,5190	0,4965	0,4393	0,3085	0,1635	0,0672
	IEF	2	3	4	6	7	6	5	3	2
	UQI	0,6773	0,6751	0,6709	0,6615	0,6375	0,5765	0,4470	0,2785	0,1326
DBA	PSNR	27,7370	24,0814	22,0566	20,4400	19,1755	18,0442	16,7126	15,3830	13,0432
	SSIM	0,9815	0,9547	0,9191	0,8768	0,8269	0,7671	0,6841	0,5800	0,4012
	IEF	20	17	16	14	14	13	11	9	6
	UQI	0,9847	0,9665	0,9433	0,9179	0,8852	0,8467	0,7860	0,7051	0,5236
BPDF	PSNR	32,0235	28,0888	25,3319	23,0051	20,8961	18,6961	16,2361	13,1205	10,2429
	SSIM	0,9757	0,9443	0,9015	0,8429	0,7674	0,6597	0,5123	0,3300	0,1984
	IEF	59	46	37	28	22	15	10	6	3
	UQI	0,9860	0,9673	0,9409	0,9030	0,8493	0,7612	0,6106	0,3759	0,1535
MDBUTMF	PSNR	35,0291	31,1976	28,6618	26,6636	24,7591	22,7032	20,0093	16,8965	13,3945
	SSIM	0,9855	0,9677	0,9442	0,9146	0,8694	0,7971	0,6538	0,4579	0,2467
	IEF	126	100	83	67	54	39	24	13	6
	UQI	0,9921	0,9819	0,9675	0,9500	0,9180	0,8742	0,7954	0,6627	0,4319
DAMF	PSNR	**35,3514**	**31,2438**	**28,7431**	26,8948	25,3174	23,9010	22,4392	20,8114	18,4485
	SSIM	**0,9864**	**0,9687**	**0,9456**	0,9185	0,8859	0,8464	0,7946	0,7203	0,5921
	IEF	**136**	**101**	**85**	72	63	53	44	35	22
	UQI	**0,9925**	**0,9822**	**0,9683**	0,9528	0,9325	0,9087	0,8765	0,8272	0,7292
NAFSM	PSNR	30,2592	27,3196	25,4859	24,1522	22,9867	21,9570	20,8512	19,6949	17,4036
	SSIM	0,9677	0,9362	0,9006	0,8635	0,8222	0,7737	0,7147	0,6389	0,5031
	IEF	42	42	41	40	38	35	31	27	17
	UQI	0,9791	0,9586	0,9359	0,9126	0,8838	0,8520	0,8108	0,7584	0,6438
AWMF	PSNR	30,8158	29,3532	28,0756	26,9417	25,6989	24,3710	22,7972	20,5303	18,7151
	SSIM	0,9685	0,9551	0,9377	0,9171	0,8908	0,8553	0,7984	0,6860	0,5992
	IEF	44	63	71	73	68	60	**48**	33	24
	UQI	0,9824	0,9745	0,9645	0,9529	0,9370	0,9159	0,8807	0,8024	0,7369
EHGA	PSNR	35,0619	30,6621	28,4056	**27,0850**	**25,7710**	**24,5242**	**22,8363**	**21,0817**	**18,9913**
	SSIM	0,9860	0,9643	0,9410	**0,9188**	**0,8913**	**0,8591**	**0,8041**	**0,7285**	**0,5935**
	IEF	127	86	77	**76**	**70**	**62**	**48**	**37**	**25**
	UQI	0,9922	0,9805	0,9666	**0,9540**	**0,9379**	**0,9192**	**0,8842**	**0,8341**	**0,7371**

Table **IV.5** shows the average PSNR, SSIM, IEF, and UQI results for AMF, DBA, BPDF, MDBUTMFG, DAMF, NAFSM, AWMF and EHGA with the ND of 50% of the images Lenna,

Cameraman, Boat, Man and Barbra. According to this Table, EHGA is more performant than all the methods except for the AWMF for Boat image. The values highlighted in bold are the best values for that noise level and the values underlined are the worst values.

Table IV.5 : Median results of the algorithms for some images in 50% ND

Image	Evaluation	AMF	DBA	BPDF	MDBUTMF	DAMF	NAFSM	AWMF	EHGA
Lenna	PSNR	22,9473	26,8136	28,1013	32,1627	33,1548	30,9516	33,4776	**33,5638**
	SSIM	0,6930	0,8884	0,8650	0,9126	0,9297	0,9054	0,9330	**0,9336**
	IEF	28	68	92	234	295	177	317	**324**
	UQI	0,6442	0,8884	0,8695	0,8966	0,9288	0,9071	0,9318	**0,9326**
Cameraman	PSNR	22,0593	26,4635	27,2624	31,6141	32,7704	29,3963	33,5201	**33,7547**
	SSIM	0,7804	0,9345	0,9026	0,9423	0,9649	0,9178	0,9683	**0,9687**
	IEF	25	69	83	226	294	135	350	**367**
	UQI	0,5818	0,8917	0,8438	0,8339	0,9384	0,8390	0,9421	**0,9436**
Boat	PSNR	21,4112	25,3246	25,9389	29,0107	29,6120	27,5709	**30,1068**	29,9520
	SSIM	0,5812	0,8328	0,8026	0,8660	0,8816	0,8416	**0,8902**	0,8880
	IEF	20	48	56	113	130	81	**144**	140
	UQI	0,5936	0,8482	0,8227	0,8680	0,8929	0,8555	**0,9029**	0,8996
Man	PSNR	22,2109	25,8922	26,9861	30,2085	30,8768	29,1792	31,1202	**31,1861**
	SSIM	0,6232	0,8570	0,8288	0,8930	0,9087	0,8665	**0,9115**	**0,9115**
	IEF	24	56	72	152	177	120	187	**189**
	UQI	0,6492	0,8826	0,8589	0,9045	0,9279	0,8900	0,9310	**0,9315**
Barbara	PSNR	19,3551	22,9639	24,1528	25,4551	25,6903	25,7796	26,3260	**26,3731**
	SSIM	0,5530	0,8149	0,8020	0,8516	0,8663	0,8470	0,8756	**0,8760**
	IEF	13	29	39	52	55	56	64	**65**
	UQI	0,6036	0,8483	0,8426	0,8677	0,8919	0,8795	0,9006	**0,9008**

Table **IV.6** shows how many times the EHGA algorithm was more performant than the other methods for PSNR, SSIM, IEF, and UQI results. It is found that, in all images, EHGA is better than the other filters for more than 90% of the comparisons.

We then gave the PSNR graph for the images Lake, Peppers, Hill, flintstones, Elaine and Couple ranging in noise densities from 10% to 90%, in Figure **IV.4**. According to these results.

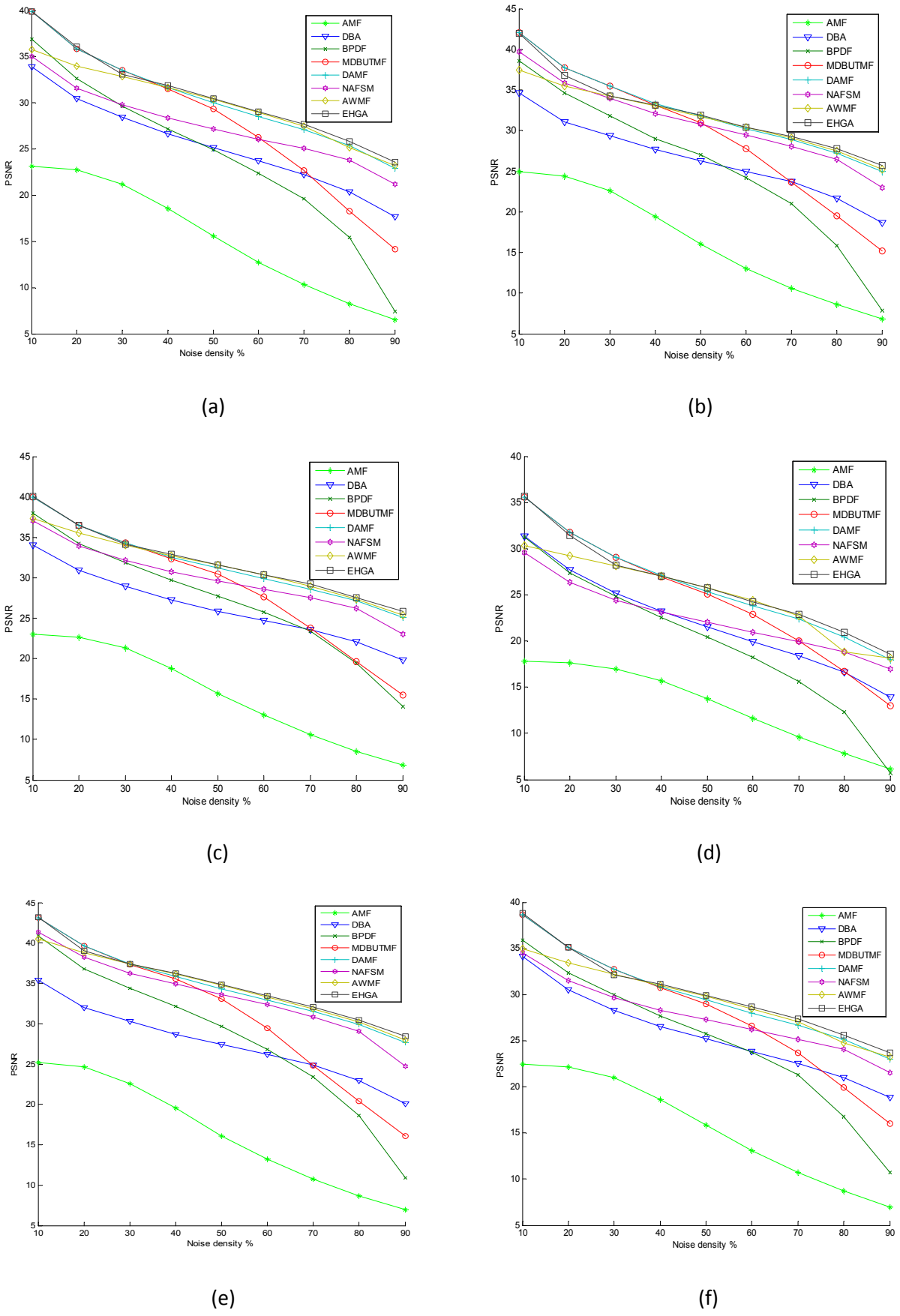

Figure IV.4 : PSNR (dB) Graph,

(a) Lake (b) Peppers (c) Hill (d) flintstones (e) Elaine (f) Couple

It can be seen that the DAMF performs well at low and medium noise densities, but fails to maintain its performance at high noise densities. The AMF performs badly at all noise densities.

In contrast, the proposed EHGA excellently outperforms other filters at most noise densities, especially for high noise densities.

Table IV.6 : Number of times that the EHGA was better than the other filters.

Image	PSNR	SSIM	IEF	IQI
Baboon	90%	90%	90%	90%
Barbara	96%	96%	96%	96%
Blonde Woman	90%	90%	90%	90%
Boat	93%	92%	92%	93%
Bridge	90%	90%	90%	90%
Cameraman	90%	92%	92%	92%
Couple	95%	95%	95%	95%
Elaine	95%	95%	95%	95%
Flintstones	90%	90%	90%	90%
Hill	94%	94%	94%	94%
Lake	95%	95%	95%	95%
Lenna	93%	92%	92%	92%
Man	93%	93%	93%	93%
Parrot	93%	93%	93%	93%
Peppers	95%	95%	94%	95%
Plane	94%	94%	94%	94%

The values obtained for PSNR, SSIM, IEF and UQI were transformed into their relative deviations between each result and the optimal value, as defined by Equation (**4.1**).

$$d(i) = \frac{r(i) - r_{ops}}{r_{worst} - r_{ops}} \tag{4.1}$$

The parameter *d* is the deviation and *r* is the result obtained for algorithm *i*, whereas r_{ops} and r_{worst} represent, respectively, the optimal and the worst possible results achieved for that metric. Since the values for the optimal and worst solutions are not always known or cannot be calculated, we can fairly consider the best and worst results from a set of values as their respective surrogates **[89]**.Therefore, for each ND, the best result within the ones obtained by the evaluated algorithms is set as r_{ops} and the worst result in this set becomes r_{worst}. These deviations were calculated for each

image and for both metrics [37]. The value 0 is the best value for that noise level and value 1 is the worst value.

According to the results of four Tables IV.7, IV.8, IV.9 and IV.10, it was found that the EHGA algorithm achieves better results than the other methods when noise levels are above 40%. In particular, EHGA is the most effective method compared to the other methods if in case of medium or high ND.

Table IV.7 : PSNR deviations for each σ for the 16 standard images

Filter	10%	20%	30%	40%	50%	60%	70%	80%	90%
AMF	1,0000	1,0000	1,0000	1,0000	1,0000	1,0000	1,0000	1,0000	1,0000
DBA	0,3165	0,3855	0,4532	0,5383	0,5860	0,5306	0,4278	0,3627	0,3482
BPDF	0,1669	0,2116	0,2724	0,3839	0,4887	0,5303	0,5313	0,6326	0,8868
MDBUTMF	0,0128	0,0035	0,0001	0,0434	0,1286	0,2606	0,3831	0,4833	0,5559
DAMF	**0,0000**	**0,0000**	**0,0000**	0,0249	0,0526	0,0561	0,0362	0,0236	0,0225
NAFSM	0,2213	0,2301	0,2353	0,2545	0,2559	0,2079	0,1439	0,0960	0,1299
AWMF	0,2198	0,1128	0,0368	0,0088	0,0049	0,0074	0,0112	0,0272	0,0033
EHGA	0,0181	0,0081	0,0277	**0,0000**	**0,0000**	**0,0000**	**0,0000**	**0,0000**	**0,0000**

Table IV.8 : SSIM deviations for each σ for the 16 standard images

Filter	10%	20%	30%	40%	50%	60%	70%	80%	90%
AMF	1,0000	1,0000	1,0000	1,0000	1,0000	1,0000	1,0000	1,0000	1,0000
DBA	0,0099	0,0290	0,0652	0,1234	0,1834	0,2012	0,1787	0,1878	0,2645
BPDF	0,0247	0,0567	0,1050	0,1838	0,2826	0,3395	0,3524	0,4560	0,7211
MDBUTMF	0,0007	0,0000	0,0011	0,0179	0,0796	0,2176	0,3974	0,5922	0,7840
DAMF	**0,0000**	**0,0000**	**0,0000**	0,0078	0,0206	0,0230	0,0132	0,0079	0,0095
NAFSM	0,0356	0,0670	0,0975	0,1335	0,1589	0,1433	0,1044	0,0853	0,1354
AWMF	0,0399	0,0249	0,0107	0,0034	0,0032	0,0042	0,0149	0,0320	0,0049
EHGA	0,0007	0,0048	0,0093	**0,0000**	**0,0000**	**0,0000**	**0,0000**	**0,0000**	**0,0000**

Table IV.9 : IEF deviations for each σ for the 16 standard images

Filter	10%	20%	30%	40%	50%	60%	70%	80%	90%
AMF	1,0000	1,0000	1,0000	1,0000	1,0000	1,0000	1,0000	1,0000	1,0000
DBA	0,7770	0,7679	0,7761	0,8098	0,8353	0,8065	0,7687	0,7570	0,7671
BPDF	0,5213	0,5232	0,5622	0,6630	0,7471	0,7935	0,8284	0,9159	0,9863
MDBUTMF	0,0590	0,0042	0,0100	0,1141	0,3000	0,5484	0,7388	0,8505	0,9041
DAMF	**0,0000**	**0,0000**	**0,0000**	0,0652	0,1235	0,1355	0,1119	0,0935	0,1096
NAFSM	0,6033	0,5232	0,4726	0,4728	0,4588	0,4129	0,3582	0,3084	0,4384
AWMF	0,6164	0,3207	0,1095	0,0272	0,0176	0,0258	0,0149	0,0467	0,0137
EHGA	0,0623	0,0253	0,0846	**0,0000**	**0,0000**	**0,0000**	**0,0000**	**0,0000**	**0,0000**

Table IV.10 : UQI deviations for each σ for the 16 standard images

Filter	10%	20%	30%	40%	50%	60%	70%	80%	90%
AMF	1,0000	1,0000	1,0000	1,0000	1,0000	1,0000	1,0000	1,0000	1,0000
DBA	0,0155	0,0366	0,0726	0,1266	0,1598	0,1518	0,1513	0,1913	0,3213
BPDF	0,0234	0,0526	0,0981	0,1757	0,2452	0,2847	0,3721	0,6215	0,9363
MDBUTMF	0,0008	0,0000	0,0036	0,0343	0,1480	0,3002	0,4295	0,5642	0,7219
DAMF	0,0008	0,0000	0,0036	0,0343	0,1480	0,3002	0,4295	0,5642	0,7219
NAFSM	**0,0000**	**0,0000**	**0,0000**	0,0086	0,0183	0,0169	0,0107	0,0074	0,0146
AWMF	0,0430	0,0756	0,1087	0,1450	0,1527	0,1252	0,1102	0,1167	0,2345
EHGA	0,0008	0,0031	0,0065	**0,0000**	**0,0000**	**0,0000**	**0,0000**	**0,0000**	**0,0000**

The results of EHGA method are presented afterward. Figures **IV.5** and **IV.6** presents the image Barbara and Bridge with the NDs (20%, 40%, 60%, 80% and 90%), respectively.

As a conclusion, it is clear that EHGA produces outstanding results at all the NDs and is always the most performant in moderate as well as high NDs.

The average PSNR, SSIM results of AMF, DBA, BPDF, MDBUTMFG, DAMF, NAFSM, AWMF and EHGA methods are presented in Figures **IV.7** and **IV.8** for image Boat and Baboon with

the ND of 60% and 80%, respectively. The values of PSNR and SSIM for the proposed method exceed the ones of the other methods.

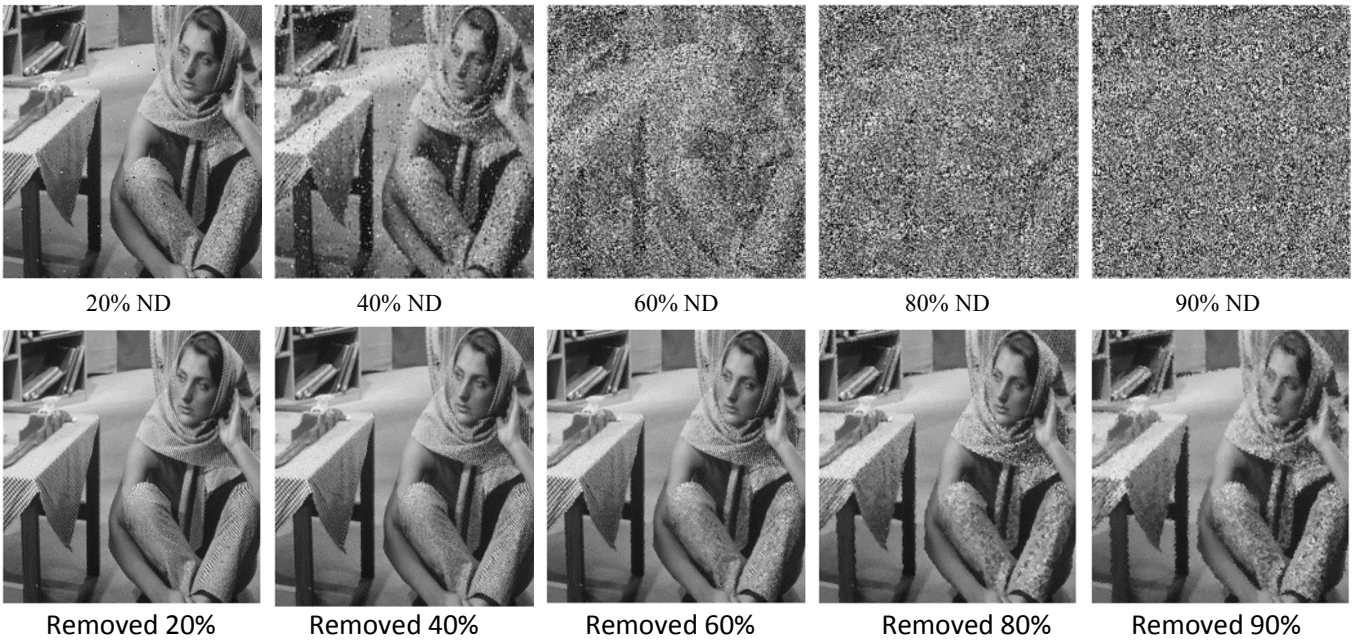

Figure IV.5 : Barbra perturbed by SPN, and Barbra images after EHGA

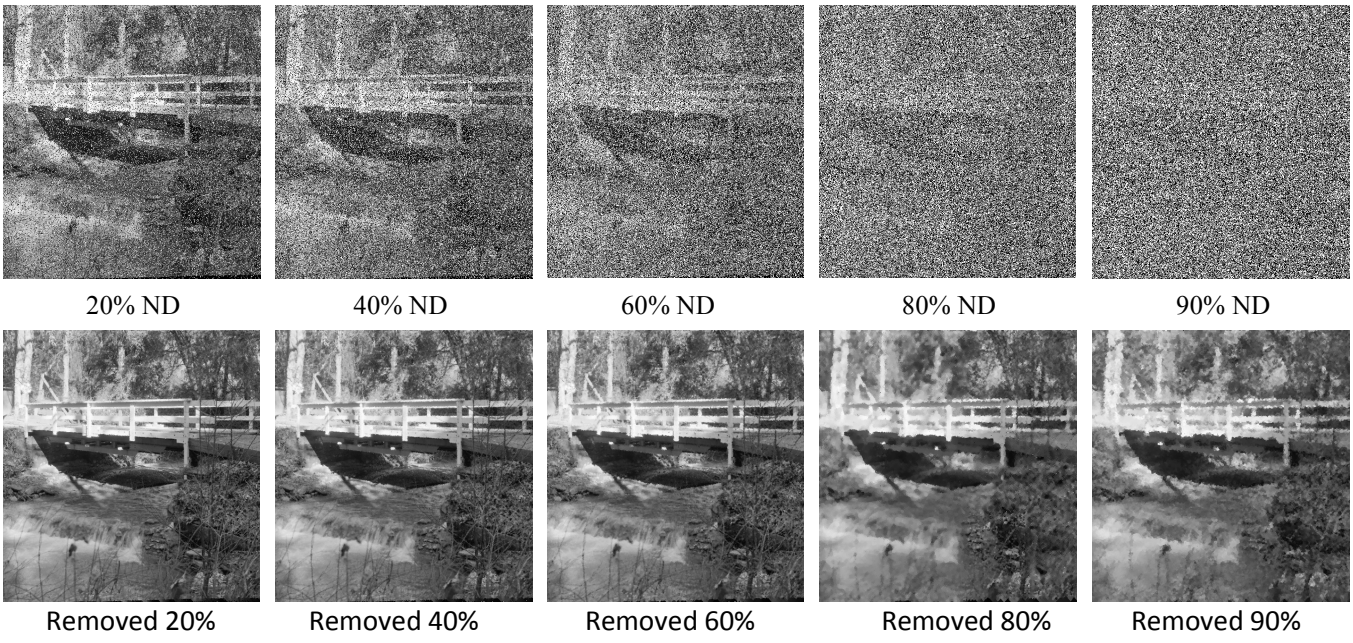

Figure IV.6 : Bridge perturbed by SPN, and Bridge images after EHGA

Figure **IV.9** gives the results of AMF, DBA, BPDF, MDBUTMFG, DAMF, NAFSM, AWMF along with the proposed method, for the image Lenna with the NDs (95, 96, 97, 98 and 99%). The results obtained by AMF, DBA, BPDF, and MDBUTMFG, are unsatisfactory and we cannot even visually identify the original image. As for DAMF, NAFSM, and AWMF, the effect of the high noise

rate can be seen in the recovered image, especially in 98 and 99%. For EHGA >70% of the image is restored and still can be visually distinguishable, even if the ND is 99% while preserving its features such as angles, edges and texture.

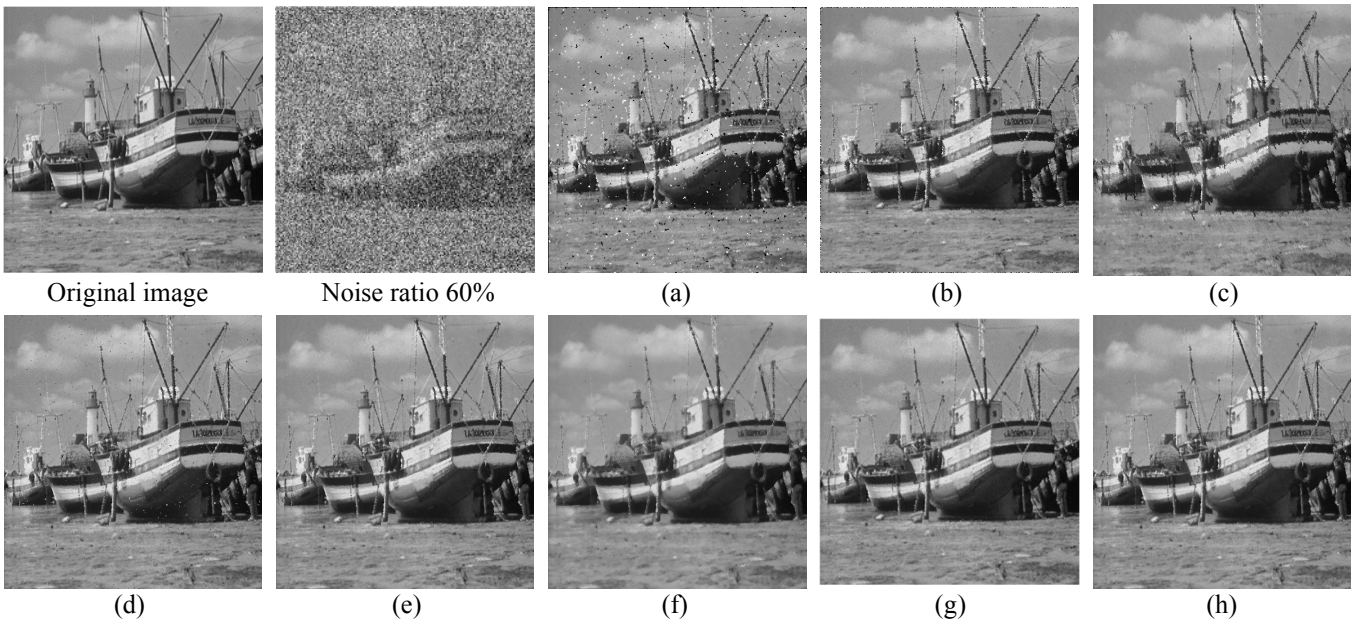

Figure IV.7 : Restoration results of Boat image.

The PSNR and SSIM are (a) AMF (19.3846 dB, 0.4853) (b) DBA (23.9898 dB, 0.7782) (c) BPDF (23.6368 dB, 0.7204) (d) MDBUTMFG (26.8627 dB, 0.7912) (e) DAMF (28.2467 dB, 0.8460) (f) NAFSM (26.4449 dB, 0.7993) (g) AWMF (28.2948 dB, 0.8487) (h) EHGA (28.6259 dB, 0.8544)

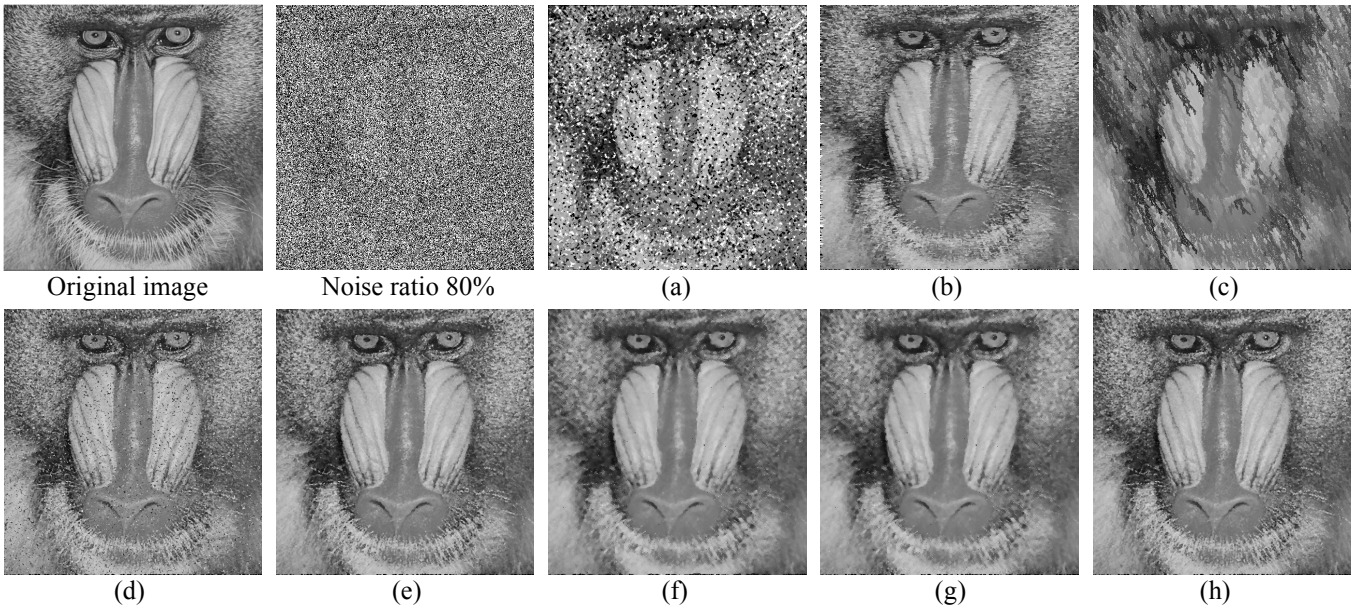

Figure IV.8 : Restoration results of Baboon image

The PSNR and SSIM are (a) AMF (11.7260 dB, 0.0990) (b) DBA (18.3770 dB, 0.4722) (c) BPDF (16.1170 dB, 0.3467) (d) MDBUTMFG (18.4298 dB, 0.4083) (e) DAMF (20.4944 dB, 0.5790) (f) NAFSM (20.4286 dB, 0.5073) (g) AWMF (20.4303 dB, 0.5086) (h) EHGA (20.6608 dB, 0.5857).

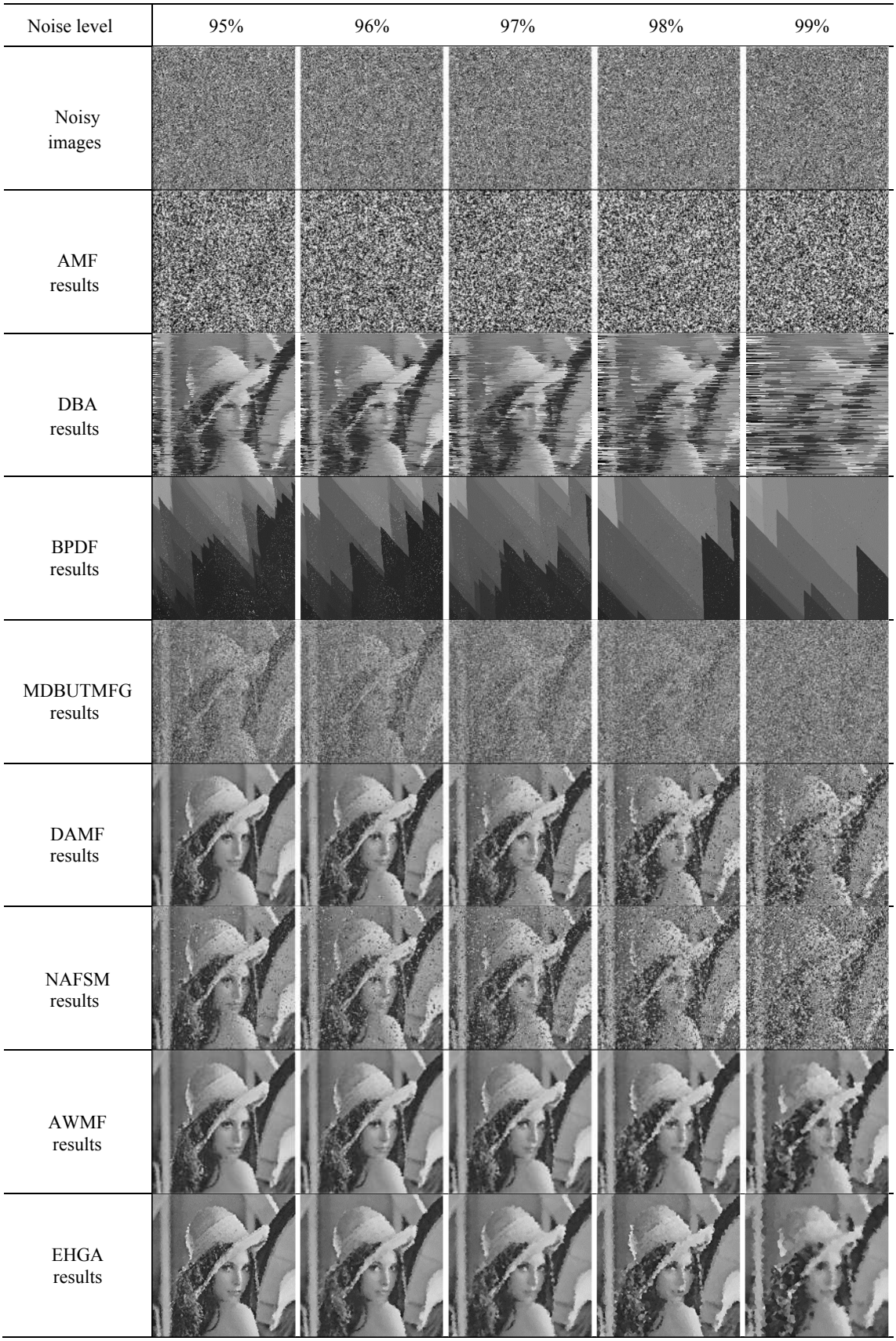

Figure IV.9 : Image filters results at different NDs

IV.6 Testing EHGA to suppress noise in medical images

The second round of tests was performed using EHGA, it was compared against different image denoising methods found in the literature to remove SPN in medical images acquired through MRI.

All of these images were corrupted with a salt and pepper noise with nine different noise densities (10, 20, 30, 40, 50, 60, 70, 80 and 90).

Original image Noisy image EHGA results

Figure IV.10 : Denoising results for Ankle image at 50% of ND.

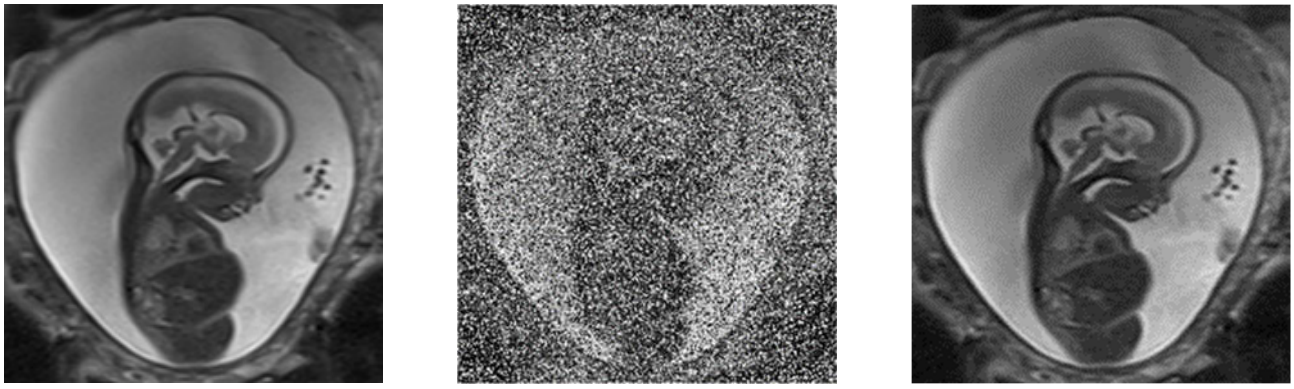

Original image Noisy image EHGA results

Figure IV.11 : Denoising results for Fetal image at 50% of ND.

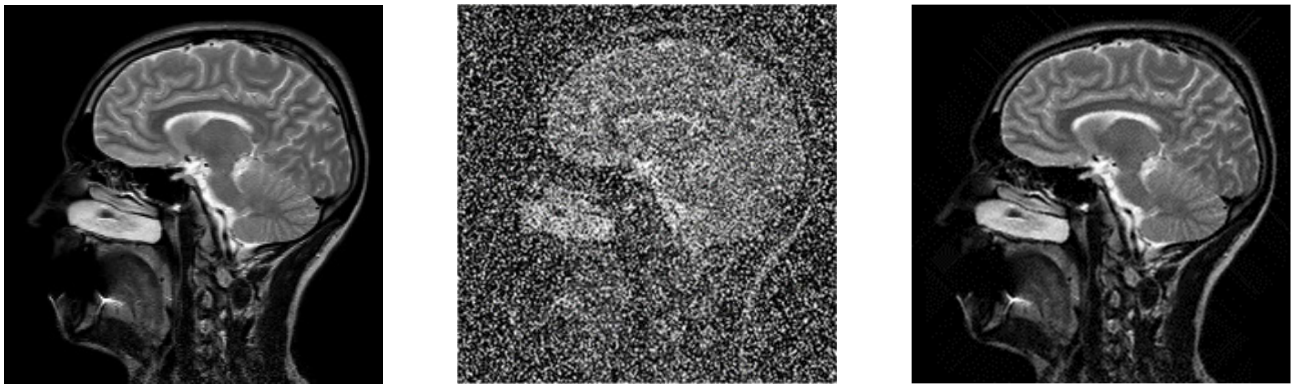

Original image Noisy image EHGA results

Figure IV.12 : Denoising results for Head image at 50% of ND.

Original image Noisy image EHGA results

Figure IV.13 : Denoising results for Knee image at 50% of ND.

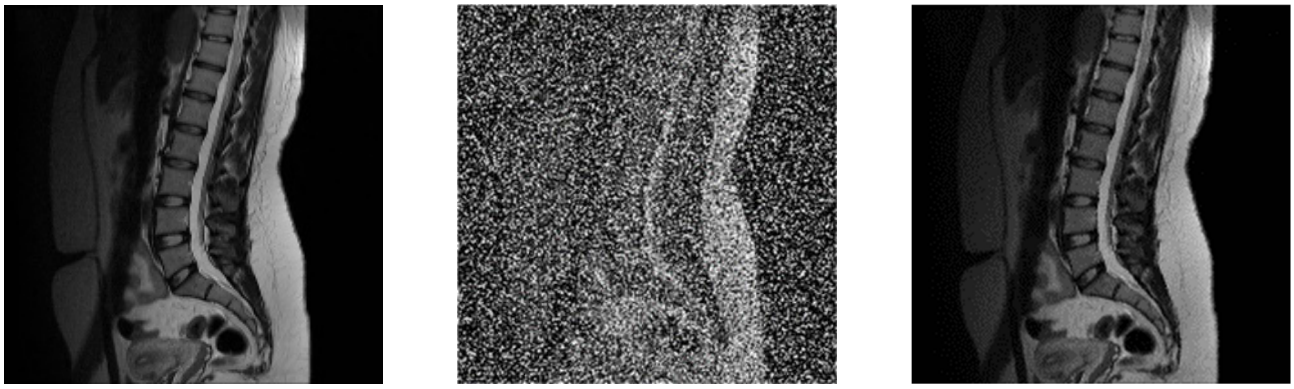

Original image Noisy image EHGA results

Figure IV.14 : Denoising results for Lumbar image at 50% of ND.

On the other hand, with the rapid development of image technology, medical images are now widely required. Hence, the proposed algorithm can also be used in the restoration of corrupted medical images. As aforementioned, the restored results presented in Figures **IV.10-IV.14** are satisfactory and robustly support the validity of our algorithm.

The six metrics mentioned in the third section are used to evaluate denoising quality. Tables **IV.11**, **IV.12**, **IV.13** and **IV.14** presents the average values of PSNR, SSIM, IEF, VIF and MSSIM of the denoising results of the methods for medical images at 60%,70% 80% and 90% of ND, respectively.

According to the obtained results, it is shown that the denoising results of EHGA, when compared to other methods, are always better.

Table IV.11 : Median results of the algorithms for medical images in 60% ND

Image	Evaluation	AMF	DBA	BPDF	MDBUTMF	DAMF	NAFSM	AWMF	EHGA
Ankle	PSNR	18.3352	12.1689	17.8049	13.2872	9.6553	12.4148	31.4293	**31.5693**
	SSIM	0.5767	0.5690	0.5820	0.4891	0.5595	0.4785	0.8538	**0.8838**
	IEF	16	4	14	5	2	4	338	**341**
	UQI	0.4251	0.5559	0.5721	0.5218	0.5811	0.5319	0.6471	**0.6771**
	MSSSIM	0.7261	0.7464	0.8545	0.6684	0.6952	0.6790	0.9750	**0.9870**
	VIF	0.1171	0.3294	0.2340	0.3626	0.4505	0.3026	0.4701	**0.4905**
Fetal	PSNR	21.9023	26.9042	29.6452	30.2919	39.3001	37.1033	40.3211	**40.3540**
	SSIM	0.6939	0.9421	0.8762	0.8718	0.9755	0.9613	0.9782	**0.9804**
	IEF	28	88	166	193	1535	926	1942	**1956**
	UQI	0.4908	0.9524	0.8844	0.7857	0.9817	0.9621	0.9757	**0.9847**
	MSSSIM	0.8123	0.9906	0.9618	0.9638	0.9969	0.9913	0.9960	**0.9973**
	VIF	0.2026	0.6322	0.4190	0.5608	0.7990	0.6379	0.8111	**0.8120**
Head	PSNR	18.5203	11.6905	22.3058	13.7858	10.2775	13.0143	31.2287	**31.2308**
	SSIM	0.5980	0.5948	0.5987	0.5176	0.6114	0.5430	0.8154	**0.8264**
	IEF	17	4	41	6	3	5	314	**318**
	UQI	0.4838	0.6189	0.6223	0.5517	0.6386	0.5991	0.7253	**0.7473**
	MSSSIM	0.7619	0.7908	0.8979	0.6963	0.7497	0.7329	0.9735	**0.9835**
	VIF	0.1243	0.3352	0.2362	0.3266	0.4494	0.3159	0.4852	**0.4972**
Knee	PSNR	18.9675	15.9022	21.1947	16.3272	13.2351	15.7840	26.9010	**26.9100**
	SSIM	0.4914	0.6994	0.6501	0.6303	0.7238	0.6488	0.8499	**0.8589**
	IEF	17	8	28	9	4	8	101	**103**
	UQI	0.4209	0.6849	0.6596	0.6586	0.7415	0.6771	0.7687	**0.7797**
	MSSSIM	0.7352	0.8996	0.8983	0.8297	0.8689	0.8470	0.9683	**0.9733**
	VIF	0.0912	0.3174	0.2424	0.3515	0.4335	0.3182	0.4505	**0.4515**
Lumbar	PSNR	20.2105	24.8025	27.7689	26.0101	33.7597	31.6529	34.2858	**34.2968**
	SSIM	0.6456	0.8915	0.8259	0.7720	0.9442	0.9090	0.9470	**0.9480**
	IEF	25	73	145	97	576	355	651	**652**
	UQI	0.3830	0.8355	0.6391	0.5235	0.9024	0.7647	0.9049	**0.9059**
	MSSSIM	0.7663	0.9777	0.9574	0.8987	0.9901	0.9797	0.9900	**0.9909**
	VIF	0.1222	0.4134	0.3061	0.3728	0.5522	0.4061	0.5572	**0.5629**

Table IV.12 : Median results of the algorithms for medical images in 70% ND

Image	Evaluation	AMF	DBA	BPDF	MDBUTMF	DAMF	NAFSM	AWMF	EHGA
Ankle	PSNR	13.6089	10.8478	19.0194	11.9345	8.9503	10.9780	29.9355	**29.9767**
	SSIM	0.3380	0.4981	0.4194	0.3948	0.5329	0.4424	0.8564	**0.8565**
	IEF	2	1	8	2	1	1	96	**97**
	UQI	0.2652	0.5178	0.4424	0.4391	0.5637	0.5045	0.6574	**0.6623**
	MSSSIM	0.5218	0.7113	0.8036	0.6157	0.6784	0.6496	**0.9806**	**0.9806**
	VIF	0.0703	0.2529	0.1459	0.2331	0.3712	0.2371	**0.4024**	**0.4024**
Fetal	PSNR	16.6232	25.6358	25.8657	24.6855	37.4687	35.1489	36.6759	**38.1769**
	SSIM	0.3820	0.9087	0.7834	0.6551	0.9642	0.9472	0.9602	**0.9693**
	IEF	8	63	67	51	963	565	802	**1134**
	UQI	0.2464	0.9239	0.7630	0.5582	0.9734	0.9450	0.9650	**0.9766**
	MSSSIM	0.5574	0.9816	0.9050	0.8775	0.9949	0.9865	0.9919	**0.9954**
	VIF	0.0923	0.5207	0.2679	0.3026	0.7259	0.5511	0.6520	**0.7369**
Head	PSNR	13.9672	10.4848	18.9554	12.4743	9.6158	11.7295	29.6120	**29.6126**
	SSIM	0.3649	0.5365	0.4880	0.4072	0.5856	0.5124	0.8025	**0.8029**
	IEF	2	1	6	1	1	1	**75**	**75**
	UQI	0.2878	0.5789	0.5040	0.4569	0.6239	0.5749	0.7330	**0.7333**
	MSSSIM	0.5613	0.7607	0.7971	0.6387	0.7351	0.7080	0.9760	**0.9763**
	VIF	0.0677	0.2560	0.1521	0.2013	0.3758	0.2555	0.4150	**0.4152**
Knee	PSNR	14.8354	15.1365	20.2040	14.8658	12.5110	14.4381	26.3032	**26.4236**
	SSIM	0.3098	0.6262	0.5588	0.5081	0.6836	0.6014	0.8115	**0.8185**
	IEF	6	6	21	6	4	5	84	**86**
	UQI	0.2650	0.6276	0.5589	0.5351	0.7106	0.6361	0.7443	**0.7490**
	MSSSIM	0.5445	0.8708	0.8398	0.7662	0.8520	0.8227	0.9594	**0.9615**
	VIF	0.0546	0.2375	0.1570	0.2221	0.3585	0.2471	0.3597	**0.3719**
Lumbar	PSNR	15.3551	23.6852	24.6728	20.9013	32.0553	30.3819	32.4905	**32.5153**
	SSIM	0.4079	0.8439	0.7306	0.5091	0.9220	0.8841	0.9259	**0.9265**
	IEF	2	15	19	8	102	69	112	**113**
	UQI	0.2031	0.7697	0.5242	0.3727	0.8690	0.7286	0.8636	**0.8729**
	MSSSIM	0.5194	0.9608	0.9085	0.7369	0.9846	0.9707	0.9853	**0.9854**
	VIF	0.0701	0.3102	0.1969	0.2130	0.4609	0.3203	0.4665	**0.4686**

Table IV.13 : Median results of the algorithms for medical images in 80% ND

Image	Evaluation	AMF	DBA	BPDF	MDBUTMF	DAMF	NAFSM	AWMF	EHGA
Ankle	PSNR	9.8582	9.2207	15.3531	10.7113	8.3621	9.9154	27.1077	**27.6334**
	SSIM	0.1369	0.4159	0.2812	0.2589	0.4868	0.3941	0.8088	**0.8111**
	IEF	1	1	3	1	1	1	50	**56**
	UQI	0.1367	0.4515	0.2664	0.3192	0.5323	0.4617	0.6309	**0.6311**
	MSSSIM	0.3174	0.6528	0.6017	0.5192	0.6536	0.6144	0.9590	**0.9646**
	VIF	0.0364	0.1714	0.0709	0.1210	0.2763	0.1681	0.2983	**0.2986**
Fetal	PSNR	12.3521	23.8349	19.9382	19.8255	35.2228	32.5663	35.3397	**35.7686**
	SSIM	0.1277	0.8482	0.5974	0.3673	0.9454	0.9188	0.9464	**0.9509**
	IEF	3	42	17	17	574	311	590	**651**
	UQI	0.1162	0.8590	0.4775	0.3547	0.9584	0.8989	0.9577	**0.9622**
	MSSSIM	0.3050	0.9558	0.7112	0.6990	0.9905	0.9761	0.9902	**0.9912**
	VIF	0.0570	0.3771	0.1252	0.1523	0.6185	0.4513	0.6110	**0.6271**
Head	PSNR	9.8503	10.4321	15.3980	10.9842	8.9767	10.5326	27.6127	**27.6426**
	SSIM	0.1421	0.4499	0.3346	0.2597	0.5415	0.4650	0.7547	**0.7555**
	IEF	1	1	3	1	1	1	47	**48**
	UQI	0.1373	0.5132	0.3188	0.3258	0.5944	0.5366	0.7061	**0.7065**
	MSSSIM	0.3272	0.7039	0.6316	0.5303	0.7116	0.6716	0.9609	**0.9611**
	VIF	0.0354	0.1724	0.0780	0.1070	0.2865	0.1892	0.3159	**0.3168**
Knee	PSNR	10.8298	14.3780	17.2435	13.2299	11.8859	13.3256	**25.5165**	**25.5165**
	SSIM	0.1231	0.5117	0.3540	0.3119	0.6177	0.5388	**0.7537**	**0.7537**
	IEF	2	5	10	4	3	4	**70**	**70**
	UQI	0.1326	0.5299	0.3537	0.3627	0.6576	0.5814	**0.6971**	**0.6971**
	MSSSIM	0.3193	0.8090	0.6885	0.6237	0.8226	0.7913	**0.9382**	**0.9382**
	VIF	0.0301	0.1500	0.0754	0.1058	0.2596	0.1684	**0.2698**	**0.2698**
Lumbar	PSNR	10.9261	21.5337	18.9062	15.9453	30.2585	28.3898	30.5810	**30.6007**
	SSIM	0.1535	0.7744	0.5424	0.2319	0.8912	0.8465	0.8951	**0.8952**
	IEF	1	9	5	2	67	44	72	**73**
	UQI	0.0974	0.6717	0.3199	0.2440	0.8260	0.6728	0.8297	**0.8299**
	MSSSIM	0.2794	0.9253	0.7164	0.5232	0.9753	0.9547	**0.9762**	**0.9762**
	VIF	0.0441	0.2070	0.0954	0.1122	0.3627	0.2364	**0.3667**	**0.3667**

Table IV.14 : Median results of the algorithms for medical images in 90% ND

Image	Evaluation	AMF	DBA	BPDF	MDBUTMF	DAMF	NAFSM	AWMF	EHGA
Ankle	PSNR	6.5839	8.7234	9.9934	9.2362	7.6871	8.7247	**24.7522**	**24.7522**
	SSIM	0.0333	0.2760	0.1275	0.1205	0.3963	0.3082	**0.7153**	**0.7153**
	IEF	0	1	1	1	1	1	**29**	**29**
	UQI	0.0474	0.3281	0.0613	0.1763	0.4604	0.3708	**0.5640**	**0.5640**
	MSSSIM	0.1383	0.5416	0.3090	0.3536	0.5967	0.5444	**0.9210**	**0.9210**
	VIF	0.0214	0.0829	0.0373	0.0539	0.1601	0.0931	**0.1727**	**0.1727**
Fetal	PSNR	8.4034	20.5338	10.2051	15.1256	30.9744	25.7858	31.8238	**31.8717**
	SSIM	0.0254	0.6944	0.1856	0.1344	0.8957	0.7999	0.9037	**0.9042**
	IEF	1	20	2	6	216	65	262	**265**
	UQI	0.0348	0.6499	0.0587	0.1693	0.9056	0.6738	0.9177	**0.9188**
	MSSSIM	0.1108	0.8529	0.2758	0.4215	0.9733	0.9202	0.9750	**0.9751**
	VIF	0.0379	0.1844	0.0420	0.0658	0.4270	0.2655	0.4329	**0.4334**
Head	PSNR	6.5735	9.9766	10.6466	9.3877	8.3203	9.3260	24.0261	**24.5820**
	SSIM	0.0375	0.3038	0.1489	0.1199	0.4559	0.3719	0.5528	**0.6620**
	IEF	0	1	1	1	1	1	21	**23**
	UQI	0.0515	0.3699	0.0726	0.1777	0.5270	0.4305	0.5707	**0.6445**
	MSSSIM	0.1442	0.5669	0.3088	0.3579	0.6567	0.5970	0.8953	**0.9141**
	VIF	0.0203	0.0821	0.0404	0.0468	0.1711	0.1072	0.1624	**0.1911**
Knee	PSNR	7.4134	13.0078	9.4196	11.2599	11.1823	12.0693	23.9885	**23.9892**
	SSIM	0.0324	0.3412	0.1089	0.1371	0.5081	0.4248	**0.6441**	**0.6441**
	IEF	1	4	2	3	3	3	**49**	**49**
	UQI	0.0534	0.3622	0.0764	0.1964	0.5654	0.4630	**0.6068**	**0.6068**
	MSSSIM	0.1461	0.6504	0.3933	0.4103	0.7647	0.7180	**0.8903**	**0.8903**
	VIF	0.0196	0.0704	0.0283	0.0462	0.1485	0.0919	**0.1552**	**0.1552**
Lumbar	PSNR	7.0840	18.5288	12.3217	11.5018	27.5005	23.4301	27.8969	**27.9238**
	SSIM	0.0320	0.6453	0.3063	0.0810	0.8297	0.7276	0.8348	**0.8352**
	IEF	0	5	1	1	36	14	**39**	**39**
	UQI	0.0322	0.4739	0.0775	0.1238	0.7319	0.4848	0.7417	**0.7421**
	MSSSIM	0.1092	0.8195	0.3469	0.3082	0.9496	0.8700	0.9519	**0.9520**
	VIF	0.0300	0.1024	0.0501	0.0546	0.2258	0.1346	**0.2283**	**0.2283**

IV.7 Conclusion

In this chapter, we have applied a novel effective hybrid genetic algorithm that removes SPN in grey images. Image quality metrics commonly used in literature are successful in verifying the performance of the approach designed with the new method and outperforming it against some modern methods.

The performance of the considered type of filters has been experienced for noise elimination from a medical image to verify the applicability of this optimal approach.

General Conclusion

Introduction

This thesis presents an effective hybrid genetic algorithm to remove salt and pepper noise. In the proposed algorithm, three different denoising methods with a genetic algorithm were used to reduce the salt and pepper noise presented in images. The initial population was generated from the three proposed methods. Then, the crossover and mutation operators were applied to create new individuals. The best individual was acquired according to the fitness function. Experimental results demonstrated that the efficiency of the effective hybrid genetic algorithm is high in comparison to different denoising methods for most salt and pepper noise ratios according to the used peak signal-to-noise ratio, structural similarity index metric, image enhancement factor and universal quality index and good detail preservation. This algorithm can work in many application fields especially medical images, such as computed tomography and magnetic resonance medical imaging.

As a consequence of the development of this work, and as previously mentioned, the results have been published in an international journal.

Contributions

The list below describes the new contributions presented in the thesis, to the best of the author's knowledge.

1. Use the genetic algorithm with the best filters to suppress the noise from the image.
2. Create a new equation based on total variation (TV) regularization term in salt and pepper noise, this function preserves important features of the image such as edges and corners.
3. Use the effective hybrid genetic algorithm (EHGA) to suppress the noise from the medical image.

Further studies

1. The proposed approach (EHGA) will be tested on 3D images.

2. Test the proposed algorithm for removing the random-valued impulse noise (RVIN).
3. Hybridization of the proposed algorithm with other optimization algorithms to achieve better results.
4. The algorithm will be applied to different types of noise such as speckle noise and Gaussian noise.
5. The proposed algorithm will be tested on colored images.
6. Computational cost may be greatly reduced.

References

[1] A. P. James and B. V Dasarathy, "Medical image fusion: A survey of the state of the art," *Inf. Fusion*, vol. 19, pp. 4–19, 2014.

[2] B. Richard and B. James, *The Handbook of Astronomical Image Processing*, 2nd editio. Willmann-Bell, 2005.

[3] A. Chrysochoos and H. Louche, "An infrared image processing to analyse the calorific effects accompanying strain localisation," *Int. J. Eng. Sci.*, vol. 38, no. 16, pp. 1759–1788, 2000.

[4] R. A. Crowther, R. Henderson, and J. M. Smith, "MRC Image Processing Programs," *J. Struct. Biol.*, vol. 116, no. 1, pp. 9–16, 1996.

[5] FACEBOOK; ERICSSON; QUALCOMM, "A Focus on Efficiency," *http://internet.org/efficiencypaper*, 2013. .

[6] L. Fan, F. Zhang, H. Fan, and C. Zhang, "Brief review of image denoising techniques," *Vis. Comput. Ind. Biomed. Art*, vol. 2, no. 1, p. 7, 2019.

[7] R. Ahmadi, J. Kangarani Farahani, F. Sotudeh, A. Zhaleh, and S. Garshasbi, "Survey of image denoising techniques," *Life Sci. J.*, vol. 10, no. 1, pp. 753–755, 2013.

[8] M. C. Motwani, M. C. Gadiya, R. C. Motwani, and F. C. Harris, "Survey of image denoising techniques," *Proc. GSPX*, pp. 27–30, 2004.

[9] D. J. Mohan. ME PhD, V. Krishnaveni, and Y. Guo, "A survey on the magnetic resonance image denoising methods," *Biomed. Signal Process. Control*, vol. 9, pp. 56–69, 2014.

[10] D. E. Goldberg, *Genetic algorithms in search, optimization, and machine learning*. 1989.

[11] P. D. I. Torino and M. Gaudesi, "Advanced Techniques for Solving Optimization Problems through Evolutionary Algorithms," no. February, 2015.

[12] Irfan Younas, "Using Genetic Algorithms for Large Scale Optimization of Assignment, Planning and Rescheduling Problems," KTH School of Information and Communication Technology SE-164 40 Kista SWEDEN, 2014.

[13] P. C. H. Chu, "A Genetic Algorithm approach for combinatorial optimisation problems," *Univ. London*, no. January, p. 181, 1997.

[14] K. K. V Toh and N. A. Mat Isa, "Noise Adaptive Fuzzy Switching Median Filter for Salt-and-Pepper Noise Reduction," *IEEE Signal Process. Lett.*, vol. 17, no. 3, pp. 281–284, 2010.

[15] U. Erkan, L. Gökrem, and S. Enginoğlu, "Different applied median filter in salt and pepper noise," *Comput. Electr. Eng.*, vol. 70, pp. 789–798, 2018.

[16] P. Zhang and F. Li, "A New Adaptive Weighted Mean Filter for Removing Salt-and-Pepper Noise," *Signal Process. Lett. IEEE*, vol. 21, pp. 1280–1283, 2014.

[17] Z.-Y. Zhu, "An Evolutionary Approach to Multi-Objective Optimization Problems," PhD thesis, The Chinese University of Hong Kong.

[18] R. C. Purshouse, "On the Evolutionary Optimisation of Many Objectives," PhD thesis, The University of Sheffield, UK.

[19] Darrell F Lochtefeld, "Multi-Objectivization in Genetic Algorithms," PhD thesis, Wright State University, 2011.

[20] J. H. Holland, *Adaptation in natural and artificial systems: an introductory analysis with applications to biology, control, and artificial intelligence*. MIT press, 1992.

[21] K. De Jong, "Evolutionary Computation : A Unified Approach Historical roots : Historical roots :

Historical roots : Present Status : Interesting dilemma : A Personal Interest : Viewpoint :," pp. 293–306, 2013.

[22] A. E. Eiben and J. E. Smith, *Introduction to Evolutionary Computing*. 2003.

[23] A. Nayyar, D.-N. Le, and N. Nhu, *Advances in Swarm Intelligence for Optimizing Problems in Computer Science"*, 1st ed. Chapman & Hall/CRC, 2018.

[24] H.-G. Beyer and H.-P. Schwefel, "Evolution strategies – A comprehensive introduction," *Nat. Comput.*, vol. 1, no. 1, pp. 3–52, 2002.

[25] X. Yu and M. Gen, *Introduction to Evolutionary Algorithms*, vol. 9, no. 4. 2010.

[26] J. Koza, "Genetic Programming: On the Programming of Computers by Means of Natural Selection," *Complex Adap. Syst.*, vol. 1, Jan. 1992.

[27] D. N. H. Thanh and S. D. Dvoenko, "IN PATTERN RECOGNITION A Method of Total Variation to Remove the Mixed Poisson Gaussian Noise 1," vol. 26, no. 2, pp. 2015–2016, 2016.

[28] M. P. Nguyen and S. Y. Chun, "Bounded Self-Weights Estimation Method for Non-Local Means Image Denoising Using Minimax Estimators," *IEEE Trans. Image Process.*, vol. PP, p. 1, Jan. 2017.

[29] S. Xu, X. Yang, and S. Jiang, "A fast nonlocally centralized sparse representation algorithm for image denoising," *Signal Processing*, vol. 131, pp. 99–112, 2017.

[30] G. Ghimpeteanu, T. Batard, and S. E. Levine, "A Decomposition Framework for Image Denoising Algorithms," no. November, 2015.

[31] V. P. Ananthi and P. Balasubramaniam, "A new image denoising method using interval-valued intuitionistic fuzzy sets for the removal of impulse noise," *Signal Processing*, vol. 121, pp. 81–93, 2016.

[32] D. Sankowski, "Noise adaptive switching median-based filter for impulse noise removal from extremely corrupted images," *IET Image Process.*, vol. 5, no. 5, pp. 472-480(8), 2011.

[33] F. Zou, "Effective and adaptive algorithm for pepper-and-salt noise removal," *IET Image Process.*, vol. 11, no. 9, pp. 709-716(7), 2017.

[34] J. Chen, Y. Zhan, H. Cao, and X. Wu, "Adaptive probability filter for removing salt and pepper noises," *IET Image Process.*, vol. 12, no. 6, pp. 863–871, 2018.

[35] M. Mafi, S. Tabarestani, M. Cabrerizo, A. Barreto, and M. Adjouadi, "Denoising of ultrasound images affected by combined speckle and Gaussian noise," *IET Image Process.*, vol. 12, no. 12, pp. 2346–2351, 2018.

[36] H. Naimi, A. B. H. Adamou-Mitiche, and L. Mitiche, "Medical image denoising using dual tree complex thresholding wavelet transform and Wiener filter," *J. King Saud Univ. - Comput. Inf. Sci.*, vol. 27, no. 1, pp. 40–45, 2015.

[37] J. L. de Paiva, C. F. M. Toledo, and H. Pedrini, "An approach based on hybrid genetic algorithm applied to image denoising problem," *Appl. Soft Comput.*, vol. 46, pp. 778–791, 2016.

[38] J. L. de Paiva, C. F. M. Toledo, and H. Pedrini, "A hybrid genetic algorithm for image denoising," in *2015 IEEE Congress on Evolutionary Computation (CEC)*, 2015, pp. 2444–2451.

[39] C. F. M. Toledo, L. de Oliveira, R. D. da Silva, and H. Pedrini, "Image denoising based on genetic algorithm," in *2013 IEEE Congress on Evolutionary Computation*, 2013, pp. 1294–1301.

[40] S. Pragada and J. Sivaswamy, *Image Denoising Using Matched Biorthogonal Wavelets*. 2008.

[41] S. Chitroub, *Principal component analysis by neural network. Application: remote sensing images compression and enhancement*. 2004.

[42] L. Chen, Y. Liu, X. Liu, and X. Wang, "A novel model to remove multiplicative noise," *J. Comput. Inf. Syst.*, vol. 9, no. 11, pp. 4223–4229, 2013.

[43] M. Malik, F. Ahsan, and S. Mohsin, "Adaptive image denoising using cuckoo algorithm," *Soft Comput.*, vol. 20, no. 3, pp. 925–938, 2016.

[44] G. Ilango and R. Marudhachalam, “New hybrid filtering techniques for removal of Gaussian noise from medical images,” *ARPN J Eng. App Sci*, vol. 6, Feb. 2011.

[45] A. Pizurica, W. Philips, I. Lemahieu, and A. Marc, “A Versatile Wavelet Domain Noise Filtration Technique for Medical Imaging,” *IEEE Trans. Med. Imaging*, vol. 22, pp. 323–331, Apr. 2003.

[46] C. Anand and J. S. Sahambi, *MRI denoising using bilateral filter in redundant wavelet domain*. 2008.

[47] M. B. Tayel, M. A. Abdou, and A. M. Elbagoury, “An Efficient Thresholding Neural Network Technique for High Noise Densities Environments,” *Elbagoury Int. J. Image Process.*, no. 54, pp. 2011–403, 2011.

[48] S. Roy, N. Sinha, and A. K. Sen, “a New Hybrid Image Denoising Method,” *Int. J. Inf. Technol. Manag.*, vol. 2, no. 2, pp. 491–497, 2010.

[49] A. Çalişkan and U. Çevik, “An efficient noisy pixels detection model for CT images using extreme learning machines,” *Teh. Vjesn.*, vol. 25, no. 3, pp. 679–686, 2018.

[50] M.-H. Hsieh, F.-C. Cheng, M.-C. Shie, and S.-J. Ruan, “Fast and efficient median filter for removing 1–99% levels of salt-and-pepper noise in images,” *Eng. Appl. Artif. Intell.*, vol. 26, no. 4, pp. 1333–1338, 2013.

[51] A. Bovik, *Handbook of Image and Video Processing*. 2005.

[52] R. H. Chan, C. Ho, and M. Nikolova, “Salt-and-Pepper Noise Removal by Median-Type Noise Detectors and Detail-Preserving Regularization,” no. November 2005, 2014.

[53] H. Ma and Y. Nie, “A two-stage filter for removing salt-Andpepper noise using noise detector based on characteristic difference parameter and adaptive directional mean filter,” *PLoS One*, vol. 13, no. 10, pp. 1–24, 2018.

[54] C.-T. Lu, Y.-Y. Chen, L.-L. Wang, and C.-F. Chang, “Removal of salt-and-pepper noise in corrupted image using three-values-weighted approach with variable-size window,” *Pattern Recognit. Lett.*, vol. 80, pp. 188–199, 2016.

[55] R. Varatharajan, K. Vasanth, M. Gunasekaran, M. Priyan, and X. Z. Gao, “An adaptive decision based kriging interpolation algorithm for the removal of high density salt and pepper noise in images,” *Comput. Electr. Eng.*, vol. 70, pp. 447–461, 2018.

[56] M. González-Hidalgo, S. Massanet, A. Mir, and D. Ruiz-Aguilera, “Improving salt and pepper noise removal using a fuzzy mathematical morphology-based filter,” *Appl. Soft Comput.*, vol. 63, pp. 167–180, 2018.

[57] V. Singh, R. Dev, N. K. Dhar, P. Agrawal, and N. K. Verma, “Adaptive Type-2 Fuzzy Approach for Filtering Salt and Pepper Noise in Grayscale Images,” *IEEE Trans. Fuzzy Syst.*, vol. 26, no. 5, pp. 3170–3176, 2018.

[58] F. Ahmed and S. Das, “Removal of High-Density Salt-and-Pepper Noise in Images With an Iterative Adaptive Fuzzy Filter Using Alpha-Trimmed Mean,” *IEEE Trans. Fuzzy Syst.*, vol. 22, no. 5, pp. 1352–1358, Oct. 2014.

[59] X. Deng, Y. Ma, and M. Dong, “A new adaptive filtering method for removing salt and pepper noise based on multilayered PCNN,” *Pattern Recognit. Lett.*, vol. 79, pp. 8–17, 2016.

[60] H. Hwang and R. A. Haddad, “Adaptive median filters: new algorithms and results,” *IEEE Trans. Image Process.*, vol. 4, no. 4, pp. 499–502, 1995.

[61] A. Pattnaik, S. Agarwal, and S. Chand, “A New and Efficient Method for Removal of High Density Salt and Pepper Noise Through Cascade Decision based Filtering Algorithm,” *Procedia Technol.*, vol. 6, pp. 108–117, 2012.

[62] S. Esakkirajan, T. Veerakumar, A. N. Subramanyam, and C. H. PremChand, “Removal of High Density Salt and Pepper Noise Through Modified Decision Based Unsymmetric Trimmed Median Filter,” *IEEE Signal Process. Lett.*, vol. 18, no. 5, pp. 287–290, 2011.

[63] U. G. Erkan and L. Okrem, “A new method based on pixel density in salt and pepper noise removal,” *Turkish J. Electr. Eng. Comput. Sci.*, vol. 263906, pp. 162–171, 2018.

[64] U. Erkan, L. Gökrem, and S. Enginoğlu, “Different applied median filter in salt and pepper noise,” *Comput. Electr. Eng.*, vol. 70, no. January, pp. 789–798, 2018.

[65] D. Zosso and A. Bustin, “A primal-dual projected gradient algorithm for efficient Beltrami regularization,” *Comput. Vis. Image Underst.*, pp. 14–52, 2014.

[66] L. I. Rudin, S. Osher, and E. Fatemi, “Nonlinear total variation based noise removal algorithms,” *Phys. D Nonlinear Phenom.*, vol. 60, no. 1–4, pp. 259–268, Nov. 1992.

[67] N. Sochen, R. Kimmel, and R. Malladi, “A general framework for low level vision,” *IEEE Trans. Image Process.*, vol. 7, no. 3, pp. 310–318, 1998.

[68] F. Dong, Y. Chen, D.-X. Kong, and B. Yang, “Salt and pepper noise removal based on an approximation of l0 norm,” *Comput. Math. with Appl.*, vol. 70, no. 5, pp. 789–804, 2015.

[69] T. CHAN and S. ESEDO, “Aspects of total variation regularized L1 function approximation,” *Siam J. Appl. Math. - SIAMAM*, Jan. 2004.

[70] L. Y. Hsu, S. J. Horng, P. Fan, H. H. Chou, X. Wang, and M. Guo, “Adaptive non-local means for image denoising using turbulent PSO with no-reference measures,” *Proc. - 2013 Int. Symp. Biometrics Secur. Technol. ISBAST 2013*, pp. 251–258, 2013.

[71] S. Kockanat, N. Karaboga, and T. Koza, “Image denoising with 2-D FIR filter by using artificial bee colony algorithm,” *INISTA 2012 - Int. Symp. Innov. Intell. Syst. Appl.*, pp. 1–4, 2012.

[72] C. Internationale, “A Differential Evolution Approach to PET Image De-noising,” no. February, 2007.

[73] V. Thavavel, J. J. Basha, M. C. Krishna, and R. Murugesan, “Heuristic wavelet approach for low-dose EPR tomographic reconstruction: An applicability analysis with phantom and in vivo imaging,” *Expert Syst. Appl.*, vol. 39, no. 5, pp. 5717–5726, 2012.

[74] K. S. @ Sankaran and N. V. Nagappan, “Noise free image restoration using hybrid filter with adaptive genetic algorithm,” *Comput. Electr. Eng.*, vol. 54, pp. 382–392, 2016.

[75] C. Shen, D. Wang, S. Tang, H. Cao, and J. Liu, “Hybrid image noise reduction algorithm based on genetic ant colony and PCNN,” *Vis. Comput.*, vol. 33, no. 11, pp. 1373–1384, 2017.

[76] J. L. de Paiva, C. F. M. Toledo, and H. Pedrini, “A hybrid genetic algorithm for image denoising,” *2016 IEEE Congr. Evol. Comput. CEC 2016*, pp. 3879–3886, 2016.

[77] D. N. H. Thanh, V. B. Surya Prasath, and L. T. Thanh, “Total Variation L1 Fidelity Salt-and-Pepper Denoising with Adaptive Regularization Parameter,” *NICS 2018 - Proc. 2018 5th NAFOSTED Conf. Inf. Comput. Sci.*, pp. 400–405, 2019.

[78] N. Alaoui, A. B. H. Adamou-Mitiche, and L. Mitiche, “Effective hybrid genetic algorithm for removing salt and pepper noise,” *IET Image Process.*, vol. 14, no. 2, pp. 289–296, 2020.

[79] D. Fajardo-Delgado, M. G. Sanchez, J. E. Molinar-Solis, J. A. Fernandez-Zepeda, V. Vidal, and G. Verdii, “A hybrid genetic algorithm for color image denoising,” in *2016 IEEE Congress on Evolutionary Computation (CEC)*, 2016, pp. 3879–3886.

[80] Z. Wang, A. C. Bovik, H. R. Sheikh, and E. P. Simoncelli, “Image quality assessment: from error visibility to structural similarity,” *IEEE Trans. Image Process.*, vol. 13, no. 4, pp. 600–612, 2004.

[81] Z. Wang and A. C. Bovik, “A universal image quality index,” *IEEE Signal Process. Lett.*, vol. 9, no. 3, pp. 81–84, 2002.

[82] H. R. Sheikh and A. C. Bovik, “Image information and visual quality,” *IEEE Trans. Image Process.*, vol. 15, no. 2, pp. 430–444, 2006.

[83] U. Erkan, D. N. H. Thanh, L. M. Hieu, and S. Enginoglu, “An iterative mean filter for image denoising,” *IEEE Access*, vol. 7, no. November, pp. 167847–167859, 2019.

[84] G. Wang, D. Li, W. Pan, and Z. Zang, “Modified switching median filter for impulse noise removal,” *Signal Processing*, vol. 90, no. 12, pp. 3213–3218, 2010.

[85] Z. Wang, E. Simoncelli, and A. Bovik, *Multiscale structural similarity for image quality assessment*, vol.

2. 2003.

[86] G. Pok and Jyh-Charn Liu, “Decision-based median filter improved by predictions,” in *Proceedings 1999 International Conference on Image Processing (Cat. 99CH36348)*, 1999, vol. 2, pp. 410–413 vol.2.

[87] U. Erkan and L. Gökrem, “A new method based on pixel density in salt and pepper noise removal,” *Turkish J. Electr. Eng. Comput. Sci.*, vol. 26, no. 1, pp. 162–171, 2018.

[88] N. Asuni and A. Giachetti, “TESTIMAGES: a Large-scale Archive for Testing Visual Devices and Basic Image Processing Algorithms,” in *Smart Tools and Apps for Graphics - Eurographics Italian Chapter Conference*, 2014.

[89] M. Chiarandini, D. Basso, and T. Stützle, “Statistical methods for the comparison of stochastic optimizers,” Jan. 2005.

Abstracts: Arabic / English / French

Abstract

Digital images are applied for a variety of purposes, from a simple family picture to disease identification in medical exams. Although image acquisition technology has evolved, every digitally acquired image has inherent noise that is usually obtained during image transfers or capture. The big challenge with this type of problems is recovering the image without losing substantial features thereof. This thesis suggests a method based on an Effective Hybrid Genetic Algorithm (EHGA) to deal with this type of problem. The EHGA integrates a genetic algorithm with some of the best image denoising methods found in the literature. The EHGA was tested on standard images and test images from Database corrupted with a salt and pepper noise for all noise densities. The EHGA was also tested with medical images that were corrupted by the same noise. The algorithm approach results, which were measured by quality metrics were compared to the results obtained by different methods. Through this hybrid approach, the EHGA was able to obtain competitive results in both types of tests, it was able even to obtain the best results in more than 90% of cases when compared to the other methods found in the literature.

Key-words:

Salt and pepper noise, medical image, genetic algorithm, hybrid genetic algorithm, image denoising.

الملخص

يَتِمّ تَطْبِيق الصُّوَر الرَّقْمِيَّة لِمَجْمُوعِه مُتَنَوِّعَةً مِنَ الْأَغْرَاضِ ، مِنْ صُورَةِ عَائِلِيَّة بَسِيطِه إِلَى تَحْدِيدِ الْمَرَضُ فِي الفحوصات الطِّبِّيَّة . عَلَى الرَّغْمِ مِنْ تَطَوَّر تِقْنِيَّةُ الْحُصُولِ عَلَى الصُّوَرِ ، إِلَّا أَنْ كُلَّ صُورَةٍ تَمّ الْحُصُول عَلَيْهَا رقميًا تَحْتَوِي عَلَى ضَوْضاء مُتَأَصِّلَةٌ يَتِمّ الْحُصُول عَلَيْهَا عادةً أَثْنَاء عَمَلِيَّات نَقَل الصُّورَةِ أَوْ التقاطها . التَّحَدِّي الْأَكْبَر مَعَ هَذَا النَّوْعِ مِنْ الْمَشَاكِل هُو اِسْتِعادَة الصُّورَةُ دُونَ فِقْدَان ميزات كَبِيرَة مِنْهَا . تقترح هَذِهِ الرِّسَالَةِ طَرِيقَة تَعْتَمِدُ عَلَى خوارزمية وِرَاثِيَّةٌ هَجِينَة فِعَالِه (EHGA) لِلتَّعامُلِ مَعَ هَذَا النَّوْعِ مِنْ الْمَشَاكِل . يدمج EHGA خوارزمية جينية مَعَ بَعْضِ مَنْ أَفْضَلِ طُرُق إِزَالَة الضوضاء بالصُّوَر الْمَوْجُودَةِ فِي الأدبيات . تَمّ اخْتِبَار EHGA عَلَى الصُّوَرِ الْقِيَاسِيَّة وَصُوَر الِاخْتِبَار مِنْ قَاعِدَةِ الْبَيَانَات التَّالِفَة بضجيج الْمِلْحُ وَالْفِلْفِلُ لِجَمِيع كَثَافَةُ الضَّوْضَاء . تَمّ اخْتِبَار EHGA أيضًا مَعَ صُوَرِ طِبِّيَّةٌ تَأَلَّفَه بِسَبَب نَفْس الضَّوْضَاء . تَمَّت مُقَارَنَة نَتَائِج نَهْج الخوارزمية ، وَالَّتِي تَمّ قِيَاسِهَا بِوَاسِطَة مَقَايِيس الْجَوْدَة ، بالنتائج الَّتِي تَمّ الْحُصُول عَلَيْهَا بِطُرُقٍ مُخْتَلِفَةٍ . مِنْ خِلَالِ هَذَا النَّهْجِ الْمُخْتَلِط ، تَمَكَّنَت EHGA مِن الْحُصُولِ عَلَى نَتَائِجَ تنافسية فِي كِلَا النَّوْعَيْنِ مِنْ الِاخْتِبَارَات ، وتمكنت حَتَّى مِنْ الْحُصُولِ عَلَى أَفْضَلِ النَّتَائِج فِي أَكْثَرِ مِنْ 90٪ مِنْ الْحَالَاتِ عِنْد مُقَارَنَتِهَا بِالطُّرُق الْأُخْرَى الْمَوْجُودَةُ فِي الأدبيات.

الكلمات الدالة:

ضَجِيج الْمِلْحُ وَالْفِلْفِلُ ، الصُّورَة الطِّبِّيَّة ، الخوارزمية الجينية ، الخوارزمية الجينية الهجينة ، تَقْلِيل ضَوْضاء الصُّورَة .

Résumé

Les images numériques sont utilisées à diverses fins, de la simple photo de famille à l'identification des maladies lors des examens médicaux. Bien que la technologie d'acquisition d'images ait évolué, chaque image acquise numériquement a un bruit inhérent qui est généralement obtenu pendant les transferts ou la capture d'images. Le grand défi avec ce type de problèmes est de récupérer l'image sans en perdre les caractéristiques substantielles. Cette thèse suggère une méthode basée sur un algorithme génétique hybride efficace (EHGA) pour traiter ce type de problème. L'EHGA intègre un algorithme génétique avec certaines des meilleures méthodes de débruitage d'image trouvées dans la littérature. L'EHGA a été testé sur des images standard et des images de test de la base de données corrompues avec un bruit de sel et de poivre pour toutes les densités de bruit. L'EHGA a également été testé avec des images médicales corrompues par le même bruit. Les résultats de l'approche algorithmique, qui ont été mesurés par des mesures de qualité, ont été comparés aux résultats obtenus par différentes méthodes. Grâce à cette approche hybride, l'EHGA a pu obtenir des résultats compétitifs dans les deux types de tests, il a même pu obtenir les meilleurs résultats dans plus de 90% des cas par rapport aux autres méthodes trouvées dans la littérature.

Mots clés :

Bruit de sel et de poivre, image médicale, algorithme génétique, algorithme génétique hybride, débruitage d'image